

Assessing the impact of land use and climate change on streamflow and nutrient delivery to the
New River Estuary, NC

A Thesis
Presented to

The Faculty of the School of Marine Science
The College of William & Mary in Virginia

In Partial Fulfillment
of the Requirements for the Degree of
Master of Science

by
Shanna C. Williamson
August 2018

APPROVAL PAGE

This thesis is submitted in partial fulfillment of
the requirements for the degree of
Master of Science

Shanna C. Williamson

Approved by committee, August 2018

Mark J. Brush, Ph.D.
Committee Chair/Advisor

Iris. C. Anderson, Ph.D.

Deborah A. Bronk, Ph.D.
Bigelow Laboratory for Ocean Sciences
East Boothbay, ME, USA

Michael F. Piehler, Ph.D.
UNC Chapel Hill Institute of Marine Sciences
Morehead City, NC, USA

TABLE OF CONTENTS

	Page
ACKNOWLEDGMENTS	iii
LIST OF TABLES	iv
LIST OF FIGURES	v
ABSTRACT	vi
INTRODUCTION	2
Freshwater Flow Regimes and Subsequent Nutrient Delivery	2
Anthropogenic Impacts on Freshwater Flow and Nutrient Delivery	3
Freshwater Flow and Nutrient Delivery Impacts on Estuarine Ecology	6
Watershed Delivery Models	7
Objectives	8
METHODS	11
Site Description	11
ReNuMa Model	13
ReNuMa Model Parameters	13
ReNuMa Model Calibration & Validation	17
Model Scaling and Simulation of Climate and Land Use Impacts	18
RESULTS	20
Model Calibration & Validation	20
Scaling to the System Level	23
Model Output: Climate and Land Use Scenarios	23
DISCUSSION	25
Model Output: Calibration and Validation	25
Model Output: Climate and Land Use Scenarios	29
Implications for the NRE Ecology	33
Summary	35
TABLES	37
FIGURES	44
APPENDICES	56
LITERATURE CITED	69
VITA	76

ACKNOWLEDGMENTS

Over the course of my academic career, I have acquired numerous mentors that played an integral part in my ability to successfully complete my graduate degree at VIMS. These mentors, who provided me with continuous encouragement and support, have in many ways become like family and will be immodestly acknowledged here. I would first like to thank my advisor, Dr. Mark “Fearless Leader” Brush. Before coming to VIMS, I was frequently told that Dr. Mark Brush was a not only a great scientist, but outstanding advisor and mentor by many of his colleagues and students. While here at VIMS, Mark has lived up to his street credentials, and exceeded my expectations for the way any advisor should interact with their students. He has provided me with an infinite amount of support, encouragement, knowledge, and smarties over the past 3 years. Additionally, his continual patience with me as I learned to balance coursework, research, and service work ensured that my time here at VIMS was challenging, but never overwhelming. His commitment to my success has truly made him the MVP of VIMS and there are not enough words in the English dictionary to thank him for all that he has done. As I venture on to the next phase of my life, I will truly miss listening out for his distinct stride on the 3rd floor of Andrews Hall. To Dr. Iris Anderson, I would like to thank you for all the knowledge, chocolate, and laughter you have bestowed upon me during my time here at VIMS. Because of you, I have learned to be exceedingly skeptical of everything I hear and read. I would also like to thank my remaining committee members, Dr. Deborah Bronk and Dr. Mike Piehler for your insight and help with my thesis research.

To my friends and support network at VIMS, I would also like to give you a huge thank you. I am especially grateful for my academic siblings, Sara Blachman and Sam Lake whose continual guidance and friendships were critical to my success at VIMS. To the members of the VIMS DiveIn committee, thank you for being another support system as we all worked to enhance diversity and inclusion on the VIMS campus. I would also like to thank my mentors and friends outside of the VIMS community. Specifically to those whom I met and adopted me as family while I was in Woods Hole, MA, thank you for all of your guidance, encouragement, and support. Your commitment to check in on my well-being while at VIMS did more for me than you could ever know.

To my family in NYC and Jamaica, I am forever grateful for your continual support to follow my childhood dreams. Thank you for reinforcing the importance of education and encouraging me to be the best me that I could be.

Finally, I would like to thank God and my extended family at the historic First Baptist Church in Williamsburg, VA. My faith keeps me grounded in this field as I am always reminded to continually examine how the research I engage in can better serve this world.

LIST OF TABLES

Table		Page
1)	Data sources used to adapt and calibrate the ReNuMa model to the NRE	38
2)	Hydrologic parameters used in ReNuMa to estimate streamflow and sediment yield.	39
3)	Nutrient parameters used in ReNuMa to estimate nitrogen and phosphorus fluxes.	40
4)	Regression statistics between Measured and Modeled Streamflow for NRE subwatersheds	41
5)	Regression statistics between Measured and Modeled TDN loads for NRE subwatersheds	42
6)	Regression statistics between Measured and Modeled TDP loads for NRE subwatersheds	43

LIST OF FIGURES

Figure	Page
1) Location and watershed boundary of the NRE, NC, MCBCL, gauging stations and associated subwatersheds used during model calibration and validation.	45
2) Schematic of (a) hydrological and (b) nutrient dynamics of the ReNuMa model (modified from Hong and Swaney 2007).	46
3) Measured and modeled streamflow for Gum Branch subwatersheds from 2008 to 2015. Top two regression plots display fits (dashed line) during calibration (top left) and validation (top right) portion of the time series while bottom regression plot displays model fit (dashed line) over entire time series. Solid line on regression plot is 1:1 line. Discharge is expressed as a yield.	48
4) Measured and modeled TDN loading for Gum Branch subwatershed from 2008 to 2015. Top two regression plots display fits (dashed line) during calibration (top left) and validation (top right) portion of the time series while bottom regression plot displays model fit (dashed line) over entire time series. Solid line on regression plot is 1:1 line. TDN loading is expressed as a yield.	49
5) Measured and modeled TDP loading for Gum Branch subwatershed from 2008 to 2015. Top two regression plots display fits (dashed line) during calibration (top left) and validation (top right) portion of the time series while bottom regression plot displays model fit (dashed line) over entire time series. Solid line on regression plot is 1:1 line. TDP loading is expressed as a yield.	50
6) Example time series plots for streamflow for MCBCL subwatersheds representing good (Cogdel), intermediate (Courthouse), and poor (Airport) fit classifications. Streamflow is expressed as a yield.	51
7) Fractional change in loads to the NRE under (a) increased temperatures, (b) changes in precipitation, (c) increased developed land (D) increased agricultural land.	52
8) Box plots of modeled change in streamflow, TDN load, and TDP load for the NRE watershed based on 24 climate projections for the 2030s, 2050s, and 2090s. The solid line within the box denotes the median of the climate projections while the whickers denote the 1 st and 3 rd quartile of the data. Data that extend beyond the whiskers are outlier points.	53
9) Fractional change in loads to the NRE under (a) decadal median climate projections for the NRE, (b) decadal median climate projections and a 25% increase in developed land, and (c) decadal median climate projections and a 25% increase in agricultural land. Median temperature increases for the NRE were 1.19, 2.31, and 4.24 °C for the 2030s, 2050s, and 2090s, respectively. Median precipitation increases for the NRE were 1.69%, 4.3%, and 9.56%, for the 2030s, 2050s, and 2090s, respectively.	54
10) Coefficient of variation between measured and modeled streamflow as a function of MCBCL watershed characteristics (a) watershed size, (b) percentage of developed and wetland area, and (c) watershed slope obtained from Piehler et al. 2017.	55

ABSTRACT

Freshwater inflow influences numerous physical, chemical, and biological characteristics of estuaries. The influx of freshwater to an estuary typically serves as an important source of allochthonous material from which primary producers derive their energy and transfer this energy to higher trophic levels. Any changes to freshwater flow subsequently impacts nutrient delivery and indirectly impacts organisms across multiple trophic levels. Anthropogenic changes to coastal land use and climate both act to threaten the integrity of estuarine systems by influencing freshwater inflow and dissolved nutrient input. Watershed loading models such as the Regional Nutrient Management (ReNuMa) model offer the ability to estimate freshwater inputs and dissolved nutrient loads to estuaries under current and future conditions. This tracking is important because it allows scientists to better understand how watershed delivery is currently impacted by anthropogenic activities and natural environmental variability, which allows for a better understanding of how watershed delivery is likely to be affected by anthropogenic changes in land use and climate.

This research aims to assess how changes in climate and coastal land cover will impact streamflow and loads of total dissolved nitrogen (TDN) and total dissolved phosphorus (TDP) to the New River Estuary (NRE), NC. We applied the ReNuMa model to the NRE watershed to estimate streamflow, TDN, and TDP loads. We used *in situ* data to calibrate (2009-2011) and validate (2012-2014) modeled streamflow and dissolved nutrient loads within 10 subwatersheds located on Marine Corps Base Camp Lejeune (MCBCL), which surrounds the estuary, and one subwatershed in the off-base portion of the NRE watershed. Following model calibration and validation, model parameters were scaled up from these subwatersheds to estimate loads from the entire NRE watershed. Model results confirm the ability of ReNuMa to capture seasonal variability in streamflow, TDN, and TDP for >50% of the subwatersheds. Under current conditions, most (71-98%) streamflow and dissolved nutrient loads are sourced from the off-base portion of the NRE watershed, while a smaller percentage of loads (2-29%) are sourced from MCBCL. Projected changes in climate revealed that changes in precipitation, even when compounded with changes in temperature, will have the greatest impact on resulting streamflow, TDN, and TDP. Streamflow and dissolved nutrient loads generally increased under anticipated climate projections through the year 2100 and such increases were further amplified under hypothetical increases in land use, especially agricultural land. Watershed delivery patterns for the NRE may therefore be substantially altered under projected changes in climate and land use. The potential impacts of changes in these loads on estuarine physical, chemical, and biological processes highlights the necessity for research assessing the impacts of land use and climate changes on watershed deli

Assessing the impact of land use and climate change on streamflow and nutrient delivery to the
New River Estuary, NC

INTRODUCTION

One of the most important factors controlling physical, chemical, and biological characteristics of many estuaries is freshwater inflow. As fresh water flows into an estuary, it carries with it watershed-derived nutrients such as nitrogen and phosphorus, both of which are necessary for algal growth which forms the base of the estuarine food web. As a result, any perturbations to freshwater inflow have the potential to affect the health of the estuary by altering nutrient inputs necessary for algal growth. Anthropogenic changes in climate and coastal land use have influenced freshwater flow regimes and watershed-derived nutrient inputs to many aquatic systems (Sklar and Browder 1998, Restrepo and Kjerfve 2000, Alber 2002, Kimmerer 2002, Knowles 2002, Magillan and Nislow 2005, Kashaigili 2008, Doll and Schmied 2012). These changes impact estuarine biogeochemical cycling and affect organisms across all trophic levels (Livingston et al. 1997, Murrell et al. 2007, Halliday et al. 2008, Baptista et al. 2010). Fortunately, watershed loading models offer a viable way to anticipate how material loads to an estuary are likely to respond to changes in climate and coastal land use. Anticipating changes to material loads has implications for achieving or maintaining a functioning estuarine ecosystem.

Freshwater Flow Regimes and Subsequent Nutrient Delivery

Freshwater inflow to an estuary varies spatially as well as intra- and interannually. Such variations in freshwater inflow are controlled predominately by estuarine vegetation as well as geographic, climatic, and topographic attributes of the adjoining watershed (Kennard et al., 2010). A freshwater flow regime, defined as the “characteristic pattern of a river’s flow quantity, timing, and variability”, may be determined by examining freshwater discharge into the estuary over the course of many years (Poff et al., 1997). Across the continental U.S., there exist two broad groups of flow regimes, intermittent and perennial, representing freshwater systems that typically have no to very low flows or freshwater systems where low to no flow days are rare

over the course of a year, respectively (Poff et al., 1989). These natural flow regimes can be further subdivided based on flow characteristics such as the magnitude of average yearly flow, the frequency and duration of flow events above a specified magnitude, the timing of flow events at a particular magnitude (i.e. seasonality), and how quickly flow changes from one magnitude to another (i.e. flash floods) (Poff et al., 1989, Poff et al., 1997). Nutrient loads to an estuary are likely to follow freshwater inflow regimes assuming that there are no major point sources of organic or inorganic material to the system. For example, in the Chesapeake Bay freshwater inflow is a reliable proxy of nutrient loading (Boynton and Kemp 2000).

Anthropogenic Impacts on Freshwater Flow and Nutrient Delivery

Land Use

As human populations have grown, there has been a general shift from predominately natural vegetation to areas characterized mostly by agricultural and urbanized land (Foley et al., 2005). Deforestation may increase watershed runoff since forested areas tend to have higher evapotranspiration rates than other vegetated land cover types (Zhang et al., 2001). Increased urban and agricultural land use types may alter freshwater inflow to estuaries by affecting processes such as infiltration and evapotranspiration (Gordon et al., 2003, Liu et al., 2008). Urbanized areas are typically characterized by high impervious surface area, which may impede soil infiltration of precipitation and result in increased runoff from land, daily discharges, and flood magnitudes (White and Greer 2006).

As freshwater inflow is altered by coastal land use this may also impact sediment and nutrient concentrations which tend to display direct relationships with freshwater inflow (Drewry et al., 2009). Increased quantities of nutrients and sediments carried from coastal watersheds to estuaries have been attributed to coastal land use change in many systems (Howarth et al. 1991,

Basnyat et al. 1999, Bowen and Valiela 2001, Weller et al. 2003). Urban and agricultural land usually increases nutrient input to an adjoining water body as a result of increased nutrient concentrations found in fertilizers, human and animal waste (Schoonover et al., 2005, Huang et al., 2013), as well as decreased nutrient retention in soils due to increased impervious surfaces (Arnold and Gibbons 1996). During the initial stages of watershed deforestation, potential increases in sediment yield can be attributed to increased soil exposure due to the direct impact of raindrops on the soil. When deforested land is converted to agricultural land however, the cultivation practices (i.e., tillage or no tillage) within that watershed may act to enhance or hinder soil erosion, resulting in increased or decreased sediment yields (Montgomery 2007).

Climate

The impact of land cover change on streamflow and nutrient delivery becomes further complicated as humans perturb the climate. Anthropogenic alterations to global air temperatures and the hydrologic cycle subsequently impact the quantity, timing, and intensity of freshwater flow and associated nutrient and sediment delivery to adjoining estuaries (Alber 2002, Doll and Schmied 2012). Global mean surface air temperatures are predicted to increase by 1-4 °C by the year 2100 (IPCC, 2007). For portions of the east coast of the U.S. (i.e., the Chesapeake Bay region), models predict on average an approximate 5 °C increase in air temperature by 2100 (Najjar et al. 2010). Unlike mean temperature which is expected to rise globally, projected precipitation patterns for the eastern United States vary depending on region and season (IPCC 2013). There is a significant amount of uncertainty among climate models regarding the way in which precipitation is likely to change for the eastern U.S. (Solomon et al. 2009). A comparative study examining precipitation pattern predictions from 22 models revealed that for most of the U.S. east coast fewer than 16 of the 22 models agreed on whether precipitation trends would

increase or decrease for every 1°C increase in temperature (Solomon et al. 2009). A more recent study examining the effects of climate change on the Chesapeake Bay found similar disagreement in model predictions, but on average suggested that precipitation in the Mid-Atlantic region is expected to increase (Najjar et al. 2010). Such increases are believed to be a result of less frequent, but more intense storm events.

As global mean temperatures increase, the resulting impact on streamflow will be largely influenced by the effect that temperature has on watershed processes such as evaporation, transpiration, and snow melt. There have been several studies conducted to investigate the effects of climate on stream runoff in the United States through the use of empirical statistical models (Revelle and Waggoner, 1983, Karl and Riebsame 1989). Studies suggesting an inverse relationship between air temperature and resulting trends in streamflow revealed the potential dominant role that evapotranspiration may have on the watershed water balance (Revelle and Waggoner 1983). There have been other studies however that question the relative importance of temperature on resulting streamflow within a watershed, suggesting that the role of evapotranspiration has been overestimated and that precipitation has a greater impact on streamflow (Karl and Riebsame 1989). Precipitation and resultant freshwater flow tend to display a direct relationship (Stogner 2000, Miao and Ni 2009, Yang et al. 2012, Liu et al., 2013). The degree to which this relationship is linear or deviates from linearity is dependent on characteristics of the watershed such as (1) dominant land cover, which impacts the proportion of water that infiltrates soils, (2) the slope of the watershed, which affects how quickly water is transported to an adjoining water body, and (3) rates of transpiration and evaporation, which impact the amount of water available for transport out of the watershed.

Potential changes in climate may act to exacerbate changes imposed by changing land use by 1) increasing nutrient concentrations in leachate that enters into groundwater as a result of increased air temperatures (Xin-Qiang et al., 2011) and 2) increasing (decreasing) the quantity of fresh water and associated nutrient inputs as a result of increased (decreased) precipitation. Given the simultaneous and interactive effects of changes in temperature, precipitation, and land use, the resulting effects on freshwater flow and nutrient delivery is typically uncertain.

Freshwater Flow and Nutrient Delivery impacts on Estuarine Ecology

Freshwater inflow affects estuarine material fluxes and physical conditions that may impact estuarine organisms across all trophic levels especially those that rely on the input of organic matter supplied from fluvial sources to derive their energy and sustain their biomass (Chanton and Lewis 2002). Increased freshwater flow increases the supply of nutrients to an estuary. Excessive nutrient input into an adjoining waterbody may stimulate excess primary production when nutrients are the most limiting resource, and induce eutrophic conditions which have become increasingly evident in much of the world's coastal waters (Cloern 2001, Selman et al. 2008). Eutrophication, defined here as an increased rate of supply of organic matter to an ecosystem (Nixon 1995), may result in further degradation of coastal water quality through (1) anoxia or hypoxia (Rabalais et al. 2001, Diaz and Rosenberg 2008), which can result in fish kills (Thronson and Quigg 2008), (2) the introduction of harmful algal species (Anderson et al., 2002), which can poison shellfish (Shumway 1990), and (3) the degradation of benthic vegetation as a result of light limitation (Short and Burdick 1996, Orth et al. 2006).

The physical conditions affected most by freshwater inflow are flushing time, stratification, and salinity. There is often an inverse relationship between freshwater inflow and flushing time (Alber and Sheldon 1999, Ensign et al., 2004). In systems characterized by long

flushing or residence times, increased freshwater flow may increase nutrient and sediment delivery to the system, but these materials may not be flushed out quickly, resulting in a further downstream shift or expansion of turbidity and chlorophyll-a maxima (Moon and Dunstan 1990). Alternatively, increased freshwater inflow may quickly flush systems of sediments and nutrients so that there is not a significant increase in the organic matter content of the system (Boyer et al. 1993). The relationship between freshwater inflow and stratification is often positively correlated (Kemp et al., 2005). Consequently, if freshwater inflow to an estuary increases, increased stratification could trap watershed-derived nutrients and phytoplankton in a more stable, illuminated surface layer, enhancing primary productivity. Alternatively, increased stratification limits vertical mixing between surface and bottom waters which may restrict nutrient and oxygen exchange between the two layers, resulting in reduced nutrient re-supply to surface waters and anoxia or hypoxia in bottom waters. The relationship between changes in streamflow and salinity varies depending on watershed characteristics and morphological properties of the estuarine basin. Alterations to salinity gradients may impact resident organisms of an estuary as demonstrated by altered fish assemblages in the Mondego estuary of Portugal (Baptista et al. 2010).

Watershed Loading Models

Models are “conceptual or mathematical simplifications (or abstractions) of a real system” (Brush and Harris 2016). Watershed models simplify the watershed processes controlling the magnitude and timing of runoff that eventually enters a nearby stream. Such models incorporate loads from point sources as well as estimates from non-point sources which are mostly driven by land cover type and local precipitation patterns. Loading models are useful for many reasons. Perhaps their most pertinent use is their ability to identify nutrient sources, the

relative contributions of these sources to total loads, and the overall magnitude of the load to a system. This tracking is important because it allows scientists to estimate current loads under current conditions which readily translate into how loading is likely to change under varying anthropogenic land use or climate change scenarios. This information has implications for management of estuarine systems and can be incorporated into development of Total Maximum Daily Loads (TMDL) (EPA, 1999).

Objectives

Intensified anthropogenic climatic variations (Dore 2005, Alexander et al. 2006), significant increases to coastal populations (Neumann et al. 2015), and changes to land use continue to impact freshwater flow and nutrient delivery to adjoining estuaries. The impact that such changes in watershed delivery are likely to have on estuarine physical, chemical, and biological components highlight the necessity for research assessing the impacts of land use and climate change on watershed material loading. As a result, the objective of this research project was to model streamflow, total dissolved nitrogen (TDN), and total dissolved phosphorus loads (TDP) to the New River Estuary (NRE) in Onslow County, NC, using the Regional Nutrient Management (ReNuMa) model. ReNuMa was calibrated and validated against measured data from 11 gauged subwatersheds within the larger NRE watershed. Following successful calibration and validation of ReNuMa to the 11 gauged subwatersheds, ReNuMa was used to predict the impacts of climate and land use change on streamflow, TDN, TDP loads to the entire NRE system. Specific objectives and hypotheses were as follows:

Objective 1: The first objective of this research was to update a prior calibration of ReNuMa in 11 subwatersheds within the NRE watershed with data that extended from 2009 to 2011 (Brush, 2013). Once calibration of ReNuMa model parameters was complete, validation of ReNuMa

output was conducted using *in situ* streamflow and dissolved nutrient loads that extended from 2012 to 2015 for five subwatersheds on MCBCL and the Gum Branch subwatershed located at the head of the NRE watershed (Fig. 1). ReNuMa model parameters were then scaled up to areas that extend beyond the subwatershed boundaries to estimate total inputs to the NRE.

Hypotheses:

1. Updating the calibration with 2009-2011 data will improve slope and r^2 values between measured streamflow and nutrient loads from the 11 subwatersheds in the NRE and ReNuMa model estimates.
2. ReNuMa model estimates for streamflow and dissolved nutrient loads will capture most of the variability in the measurements.
 - Since ReNuMa was created for relatively large watersheds ($\sim 10^3$ km²) with mixed land cover types, comparisons between data and ReNuMa modeled output for the Gum Branch station will display a relatively high coefficient of determination and a slope that is not statistically different from 1. The 10 subwatersheds that are on MCBCL are two orders of magnitude smaller than the size of watersheds that ReNuMa is designed for and are less diverse in land cover types. As a result, ReNuMa will capture much less of the variability in measured streamflow when compared to the larger Gum Branch station.

Objective 2: The second objective was to run a series of different but likely temperature, precipitation, and land use “What if?” scenarios to determine how freshwater flow and dissolved nutrient loads are likely to change under anticipated changes in land use and climate for the NRE watershed.

Hypotheses:

1. Under increased agricultural and urbanized land use projections for the NRE, inputs of fresh water and dissolved nutrients are expected to increase.
2. Under increased precipitation projections for the NRE, inputs of fresh water and dissolved nutrients are expected to increase, while the opposite will be true under decreased precipitation projections.
3. Under increased temperature projections for the NRE, streamflow is expected to decrease as a result of increased evaporation across different land cover types. Increased temperatures may increase leaching of nutrients into water as it passes through the watershed, but decreased streamflow will result in an overall decrease in dissolved nutrient loads.
4. Under simultaneous decreased precipitation and increased temperature for the NRE, streamflow is expected to decrease. Nutrient loads are expected to be influenced more by precipitation than temperature. As a result, any potential increases in dissolved nutrient loads as a result of increased temperature will be negated by potential decreased dissolved nutrient loads resulting from decreased precipitation and streamflow.
5. Under simultaneous increased precipitation and increased temperatures for the NRE, streamflow trends are uncertain and will be dependent on rates of evapotranspiration, but are still expected to increase. Dissolved nutrient loads are expected to increase as well.

METHODS

Site Description

The New River Estuary (NRE) is a relatively small ($\sim 64 \text{ km}^2$), shallow (average depth $\sim 1.8 \text{ m}$), semi-lagoonal estuary in Onslow County, NC (Brush 2013) (Fig. 1). The mouth of the NRE is characterized by a series of barrier islands which restrict flow between the estuary and Atlantic Ocean. Such flow restriction is responsible for the microtidal nature of the NRE and is partially responsible for the relatively long freshwater flushing time which averages approximately 70 days (Ensign et al. 2004, Brush 2013, Pearl et al. 2013).

The adjacent NRE watershed is approximately $1,436 \text{ km}^2$ and is characterized by a mixture of land use types including forested (41.5%), wetland (28.3%), open water (0.4%), agricultural (14.5%), and developed areas (14.3%); these distributions have not changed substantially between 2006 and 2011. Agricultural areas are confined mostly to the upper region of the watershed and include both row crops and confined animal feeding operations primarily for hogs (Brush, 2013). The lower watershed is a relatively low-relief, predominately developed region as most of it lies on Marine Corps Base Camp Lejeune (MCBCL), although some forested and wetland areas exist on the base. Most of the population in the lower watershed is connected to sewer lines while the population on septic systems is predominately in the upper watershed.

Nutrient inputs to the NRE originate from several major sources including direct atmospheric deposition, groundwater, riverine discharge, and a wastewater treatment plant that discharges sewage effluent into the middle of the estuary from MCBCL (Brush 2013). Previous studies examining the influence of climatic variations on physical, chemical, and biological components of the NRE revealed that changes in riverine discharge strongly influence flushing time, water column irradiance through increases in total suspended solids and chromophoric

dissolved organic matter (CDOM), and nutrient inputs into the estuary (Peierls et al. 2012, Brush 2013, Anderson et al. 2014).

The dominant forms of inorganic nutrients entering the NRE during increased freshwater flow are nitrate and phosphate (Peierls et al. 2012, Hall et al. 2013). Inorganic nutrient concentrations tend to be highest at the head of the estuary since most allochthonous nitrogen and phosphorus are sourced from the upland, off-base portion of the NRE watershed (Brush 2013). These nutrient additions typically stimulate phytoplankton blooms in the upper estuary, which are particularly sensitive to discharge-induced variations in flushing time (Peierls et al. 2012). As freshwater flows down the axis of the NRE, inorganic nutrient concentrations are controlled less by input from the watershed and more so by the recycling of organic matter (Anderson et al., 2014). During periods of low freshwater flow, inorganic nutrient concentrations both at the head and along the axis of the NRE tend to be low. This contrasts with periods of relatively high freshwater flow, which pushes inorganic nutrients further downstream and increases inorganic nutrient concentrations along the entire NRE axis (Peierls et al. 2012).

The upper, off-base portion of the watershed is gauged at a U.S. Geological Survey (USGS) station on the New River at Gum Branch, NC (station 02093000, Fig. 1). Discharge at Gum Branch over the study period was monitored daily by the USGS, while nutrient concentrations were collected on a monthly basis and during selected storms from 2008 to 2015 (Weyers, 2013, Ensign, 2017). Monthly nutrient loads from Gum Branch were determined by first computing loads for each date on which nutrient concentrations were measured and then combining flux-flow regressions with daily discharge to compute daily loads. The daily loads were then summed to arrive at monthly estimates. Monthly discharge and nutrient loads from 10

gauged subwatersheds on MCBCL were quantified by Piehler et al. (2017a, b) and provided by the author.

ReNuMa Model

Watershed models offer the ability to estimate freshwater, nutrient and sediment loads into estuaries. The Regional Nutrient Management (ReNuMa) Model estimates surface runoff, sediment transport, streamflow, and nutrient fluxes from point sources, groundwater and surface runoff (Fig. 2) (Hong and Swaney 2007). ReNuMa is based on two previously developed models: the Generalized Watershed Loading Functions (GWLF) model, which estimates nutrient and sediment flow through different land covers and subsurface zones of the watershed, and the Net Anthropogenic Nitrogen Inputs (NANI) model, which estimates anthropogenic nitrogen inputs to the watershed. ReNuMa builds off of the GWLF and NANI models by accounting for additional nitrogen transformation processes as it percolates through different land covers and exits the watershed. These additional nitrogen transformation processes include in-river and sewage denitrification, and percolation of atmospherically-deposited nitrogen through land use types accounting for seasonal changes in precipitation (Hong and Swaney 2007). Estimates for streamflow, nutrient fluxes, and sediment transport are based on empirical observations and mass balance using well established relationships between measurable parameters. For example, sediment erosion and transport are calculated using the Universal Soil Loss Equation (USLE), which requires a soil curve number obtained from the Soil Conservation Service (Hong and Swaney 2007).

ReNuMa Model Parameters

The application of ReNuMa to a study area requires processing of several data sets (Table 1). Estimates of streamflow and sediment delivery utilize the hydrologic dynamics of the

ReNuMa model (Fig. 2). The hydrologic model relies on mass balance of several transport parameters (Table 2) as well as empirical data such as daily precipitation and average air temperature. The calculations for the transport parameters also rely on land cover and soil properties of the NRE. Estimates of watershed nutrients entering the estuary via streamflow utilize the nutrient dynamics of the ReNuMa model (Fig. 2). Nutrient input sources for the watershed are derived from point sources such as sewage facilities, as well as several non-point sources such as atmospheric nitrogen deposition, nutrient concentrations estimated for different land covers of the watershed (adjusted for plant uptake and denitrification), groundwater nutrient input, and loads from septic systems (Table 3).

Hydrologic Parameters

Climate input data were derived from 25 historical surface observation stations with daily measurements of precipitation (mm) and air temperature (max. and min., °C) across eastern NC (Wooten et al., 2017). Daily minimum and maximum air temperatures were averaged to obtain an estimate of daily mean temperature. A spatial average of these daily measurements spanning from 2007 to 2015 were used as daily climate input data for ReNuMa.

Dominant land cover types within the 11 subwatersheds and for the entire NRE were determined in ArcMap using shapefiles obtained from the National Land Cover Database (NLCD) for the years 2006 and 2011 (Fry et al., 2011, Homer et al., 2015). ReNuMa allows for estimation of anthropogenic nutrient inputs from several different agricultural class areas. This is useful because one can specify loads from agricultural areas resulting from fertilizer and manure application, which is dependent on the type of crop used in the NLCD agricultural land classification. As a result, areas classified as ‘Cultivated Crops’ by the NLCD were split into soybean (39%), corn (33%), cotton (17%), and wheat (11%) based on the percent contribution of

each crop at the county level (USDA-NASS 2000-2008).

ReNuMa hydrologic transport parameters are outlined in Table 2. The recession coefficient which is defined as the rate at which total flow returns to base flow following a relatively high precipitation event was calculated using daily discharge data from the 11 subwatersheds between the years 2008 and 2011. Nine precipitation events in each subwatershed were selected between 2008 and 2011, and the natural log of discharge over the time taken to return to base flow was regressed over time, with the slope representing the recession coefficient for the specific precipitation event. Recession coefficients determined for the nine precipitation events in each subwatershed were averaged. The seepage coefficient represents the proportion of water in the shallow saturated zone of the aquifer that makes it to the deep aquifer (Fig. 2a). For most watersheds, we adopted a conservative approach for this parameter and used a value of zero. There were, however, some watersheds that have values greater than zero for this parameter as determined using the autocalibration function of ReNuMa. The dimensionless sediment delivery ratio (SDR) is the ratio between the amount of sediment entering a watershed and the amount of sediment lost to erosion. This parameter was calculated using the Vanoni (1975) equation,

$$SDR=0.451(b^{0.298})$$

where b is the size of the watershed area in square kilometers.

Default ReNuMa values were used to initialize saturation conditions of the watershed soils and antecedent moisture conditions, which were then estimated by the model during a one-year spin-up period prior to the calibration. Unsaturated storage water capacity refers to the subsurface water depth that is within the root zone of surface plants; the default ReNuMa value of 10 cm was used for this parameter. Erosivity coefficients, which are used to calculate erosion for different surfaces, were derived from reference tables in Selker et al. (1990) by season. Evapotranspiration cover coefficients estimate the

quantity of water loss during evaporation and transpiration in the watershed. This parameter should range in value between zero and one and approaches a value of one as plants approach full foliage. This parameter was estimated using land cover type data and approximate values for evapotranspiration cover coefficients outlined in tables in the GWLF user's manual (Haith et al. 1992).

Both the runoff curve number and Universal Soil Loss Equation (USLE) parameter were derived from soil characteristics data obtained from the National Resources Conservation Service (NRCS) Soil Survey Geographic (SSURGO) database and processed using ArcMap. Runoff curve numbers estimate runoff potential from a watershed and range from 30 to 100, with higher numbers indicating greater runoff potential and lower numbers indicating low runoff potential. Values are based on soil group type and land cover information. SSURGO classifies soils in four hydrologic soil group types represented by the letters A-D, with the characteristics of each soil group type ranging from well drained to poorly drained. Runoff curve numbers for each watershed were obtained from NRCS tables in the GWLF user's manual (Haith et al., 1992) as a function of soil group type and land cover.

The USLE parameter is the product of four separate parameters based on land cover. The four parameter values include K , the soil erodibility factor, LS , a topographic factor, C , a cover management factor, and P , a supporting practice factor. K was obtained from SSURGO data. The LS factor was calculated by multiplying slope length of each watershed by percent slope. A 20 foot Digital Elevation Model (DEM) GIS coverage obtained from the USGS National Elevation Dataset was used to calculate slope length for each land use type using the 'Flow Length' tool in ArcMap, while application of the 'Slope' tool in ArcMap allowed for calculation of the percent slope for each land use type (Hickey 2000). The GWLF user's manual provided reference tables for determining the C and P parameters (Haith et al., 1992). Since the USLE parameter value estimates soil loss, values of zero were used for land cover types that were classified as barren, wetlands, open water, and developed/urban.

Nutrient Parameters

ReNuMa nutrient parameters are outlined in Table 3. Nutrient input data were derived mainly from reference tables in the GWLF user's manual (Haith et al., 1992), which provided national maps of typical sediment nutrient content within surface soils (top 30 cm) and reference tables for dissolved nutrient concentrations in forested and agricultural runoff and groundwater discharge, as well as nutrient accumulation rates in urban areas. Point source discharges were obtained from the Environmental Protection Agency (E.P.A.) Water Discharge Permits website (NPDES, www.epa.gov/npdes). In order to estimate loads from septic systems, we estimated the percentage of the population using septic systems as opposed to the percent connected to public sewers. For watersheds in the lower half of the NRE watershed on MCBCL, we assumed that none of the population is on septic. For the upland area of the NRE watershed, we obtained a GIS shapefile outlining sewer service area in the watershed in 2004 (NCCGIA 2007) and merged that shapefile with population data by census block from the US Census Bureau Topologically Integrated Geographic Encoding and Referencing (TIGER) database. We subtracted the number of people outlined in the sewer service areas from the total population in the upland area of the watershed and assumed the remaining population was using normal septic systems. Annual septic nitrogen and phosphorus inputs were calculated assuming $4.8 \text{ kg N person}^{-1} \text{ y}^{-1}$ (Valiela et al. 1997) and $0.34 \text{ kg P person}^{-1} \text{ y}^{-1}$ (Alhajjar et al. 1989), respectively.

ReNuMa Model Calibration and Validation

ReNuMa was visually calibrated to observed monthly discharge and loading of TDN and TDP from 2008 to 2011. During calibration, several hydrologic parameters including recession and seepage coefficients and unsaturated storage water capacity were adjusted for all subwatersheds within reasonable bounds outlined in the ReNuMa user's manual, occasionally making use of ReNuMa's autocalibration tool (Hong and Swaney 2007). Following calibration,

ReNuMa model output was validated using monthly discharge and loading data from 2012 to 2015. In order to quantitatively assess how well model output reflected observed data, several statistical metrics were computed including mean and median absolute error, mean and median percent error, and root mean squared error. Additionally, linear regressions between observed data and model output allowed us to assess if the slope and intercept were significantly ($p < 0.05$) different from one and zero, respectively, and if ReNuMa model output captured a significant ($p < 0.05$) amount of the variability in the data for the calibration period, validation period, and overall time series.

Before beginning a statistical assessment of ReNuMa modeled output for streamflow, TDN and TDP, three fit classification categories were defined for good, intermediate, and poor fits between measured and modeled data. The regression line between ReNuMa modeled and measured data for good fits would require a slope not significantly different from 1 ($p < 0.05$) and an overall model fit that was significantly different from 0 ($p < 0.05$). Intermediate fits would be regression lines that had slopes significantly different from 1, but an overall model fit that was significantly different from 0 ($p < 0.05$). Poor fits were defined as regression lines with overall model fits that were not significantly different from 0.

Model Scaling and Simulation of Climate and Land Use Impacts

Once calibration and validation were complete, ReNuMa was used to compute average annual loads to the NRE from both the upper, off-base portion of the NRE watershed as well as from the on-base portion of the watershed on MCBCL (Fig. 1). Parameter values obtained during the calibration of the Gum Branch watershed were used for the off-base portion of the watershed. The median of parameter values obtained during the calibration of the 10 on-base subwatersheds were used for the MCBCL portion.

Wooten et al. (2017) developed an ensemble of 24 climate projections for potential changes in air temperature and precipitation through 2100 for the NRE watershed. Brush et al. (2018) summarized these 24 projections and reported first, second and third quartiles of predicted temperature warming by 2100 of 3.8, 4.2, and 5 °C, respectively, with minimum and maximum changes of 2.6 and 7.8 °C, respectively. The first, second, and third quartiles of percent change in precipitation by 2100 were -5, 10, and 14% relative to current conditions, respectively, with minimum and maximum changes of -27% and +31%, respectively. Brush et al. (2018) also summarized projections for the 2030s, 2050s, and 2090s. The individual impacts of changes in air temperature, precipitation, and land use on modeled streamflow and nutrient loads were first tested by running ReNuMa after increasing air temperatures from +1 to +5 °C based on the 2100 projections above, changing precipitation from -20% to +20% of current values, again based on the projections above, and hypothetically increasing developed and agricultural land individually by 10%, 25%, and 50%. To obtain more realistic projections of streamflow and nutrient loads under the combined influence of temperature warming and changes in precipitation, ReNuMa was then run using all 24 climate projections for the 2030s, 2050s, and 2090s. Finally, hypothetical increases in developed and agricultural land use were superimposed on the median climate projections for the 2030s, 2050s, and 2090s.

RESULTS

Model Calibration & Validation

Gum Branch Subwatershed

Successful application of ReNuMa to the subwatersheds of the NRE was the first of two objectives for this research. Across the eleven subwatersheds, ReNuMa model output most closely matched the observations for Gum Branch. This subwatershed together with the portion of the watershed below the gauge serves as the major source of fresh water and dissolved nutrient loads to the NRE owing in large part to its size and location in the most upland portion of the NRE watershed, where land use is heavily influenced by agriculture (Brush, 2013, Fig. 1). Compared to the MCBCL subwatersheds, ReNuMa model output for Gum Branch during the calibration period consistently captured the greatest variability in measured streamflow (70%), TDN (64%), and TDP (70%) (Figs. 3-5). Slightly lower r^2 values resulted for the validation period (approximately 0.6, 0.6, and 0.5, respectively). Overall model fits for Gum Branch streamflow, TDN, and TDP had r^2 values greater than 0.5 and equated to good fit classifications for streamflow and TDN, and an intermediate fit classification for TDP (Tables 4-6).

MCBCL Subwatersheds: Overview

For the ten MCBCL subwatersheds, ReNuMa model output was quite varied as represented by the number of good, intermediate, and poor fits for streamflow, TDN loads, and TDP loads (Tables 4-6). Overall, across all MCBCL subwatersheds, ReNuMa did the best at modeling streamflow, followed by TDN, and finally, TDP. The results from a statistical assessment of fits across all MCBCL subwatersheds are discussed below for each variable.

MCBCL Subwatersheds: Streamflow

Statistical assessment of measured versus modeled streamflow data revealed that out of the ten MCBCL subwatersheds used to calibrate and validate ReNuMa, five of these watersheds had good overall model fits (Table 4). These good fits were for two subwatersheds where data extended only through the calibration period (Freeman and Gillets) and three subwatersheds where data extended the entire research period (Cogdels, French, and Tarawa). For these good model fits, ReNuMa captured anywhere from 8 to 53% of the variability in the measured data (Table 4). There were three watersheds that received intermediate fit classifications for streamflow. The data for two of these watersheds extended the entire research period (Courthouse and Traps) while the data for one watershed extended to the end of the calibration period (Camp Johnson). ReNuMa captured anywhere from 17 to 58% of the variability in these watersheds (Table 4). The two watersheds with poor fits (Airport and Southwest) had data that extended to the end of the calibration period. The variability captured by ReNuMa for these two watersheds ranged from 7 to 9% (Table 4). Time series plots for good fits typically displayed good overlap of measured and modeled data and highlighted the ability of ReNuMa to capture most of the monthly and interannual variability in measured loads (Fig. 6). For watersheds that were classified with intermediate fits, ReNuMa typically displayed good overlap of measured and modeled data over the entire time series, but did not always capture interannual variability, especially during the validation period (Fig. 6). For watersheds that were classified with poor fits, ReNuMa was not able to capture the variability in the data nor did ReNuMa output overlap measured loads well over the length of the time series (Fig. 6). Model output for good, intermediate, and poor fits for all MCBCL subwatersheds for streamflow, TDN, and TDP are available in the Appendix.

MCBCL Subwatersheds: TDN Loads

Three of the ten MCBCL subwatersheds had good model fits for TDN load. These good fits included two watersheds (Cogdels and French) where data extended the entire research period and one watershed (Freeman) where data only extended through the calibration period. For these good model fits, ReNuMa captured anywhere from 10 to 53% of the variability in the measured data (Table 5). There were five watersheds with intermediate model fits. The data from three of these watersheds extended the entire research period (Courthouse, Tarawa, and Traps) while two watersheds extended to the end of the calibration period (Camp Johnson and Gillets). ReNuMa captured anywhere from 9 to 51% of the variability in these watersheds (Table 5). The data from the two watersheds with poor fit classifications (Airport and Southwest) only extended to the end of the calibration period. The variability captured by ReNuMa for these two watersheds ranged from 6 to 8% (Table 5).

MCBCL Subwatersheds: TDP Loads

Only one MCBCL subwatershed had a good model fit classification for TDP load. This good fit was the Freeman watershed where data only extended through the calibration period and where ReNuMa captured approximately 63% of the variability in the measured data. There were six watersheds with intermediate model fits, five of which had data that extended the entire research period (Cogdel, Courthouse, French, Tarawa, and Traps) and one watershed where data extended to the end of the calibration period (Camp Johnson). ReNuMa captured anywhere from 11 to 54% of the variability in these watersheds. There were three watersheds with poor fits all of which only extended to the end of calibration period (Airport, Gillet, and Southwest). The variability captured by ReNuMa was less than 1% for these subwatersheds.

Scaling to the System Level

At the system level, ReNuMa estimated that approximately 71% of freshwater inputs to the NRE are sourced from the off-base portion of the watershed while approximately 29% are derived from MCBCL. ReNuMa estimated that approximately 97% of TDN loads are sourced from the off-base portion of the watershed while only 3% are sourced from MCBCL. Similarly to TDN, ReNuMa estimated that approximately 98% of TDP loads are sourced from the off-base portion of the watershed while only 2% are sourced from MCBCL. These estimates identify the off-base portion of the watershed as the dominant source of freshwater and dissolved loads to the estuary and are consistent with estimates from other watershed loading models that have been applied to NRE watershed (Brush 2013). These previously applied models estimated that the off-base portion of the watershed contributes anywhere from 61 to 93% and 34 to 95% of TDN and TDP loads, respectively (Brush 2013).

Model Output: Climate and Land Use Scenarios

Individual Impacts of Climate and Land Use on Loads

Increasing air temperature in 1 °C increments up to a maximum of 5 °C for the entire NRE watershed resulted in decreased inputs of freshwater, TDN, and TDP (Fig. 7a). At the maximum 5 °C increase, streamflow and loads of TDN and TDP decreased by 9.6, 6.3, and 8.3%, respectively. Modeled streamflow, TDN loads, and TDP loads were positively correlated with changes in precipitation (Fig. 7b). That is, as precipitation increased (or decreased), streamflow, TDN, and TDP also increased (or decreased). A 20% increase in precipitation resulted in a 35.0, 24.0, and 52.2% increase in streamflow, TDN, and TDP, respectively, while a 20% decrease in precipitation caused a 25.6, 16.9, and 35.2% decrease in the same variables.

Increasing developed land by 10, 25, and 50% resulted in small (< 1%) increases in streamflow and TDN loads and decreases in TDP loads (Fig. 7c). Increasing agricultural area by 10, 25, and 50% resulted in only small (~1%) increases in streamflow, but much larger increases in TDN and TDP loads, with maximum increases of 23.1 and 49.4%, respectively (Fig. 7d).

Cumulative Impacts of Climate and Land Use on Loads

Running the 24 climate projections with simultaneous changes in temperature and precipitation resulted in median 6.4, 5.8, and 16.2 % increases in streamflow, TDN, and TDP loads by the year 2100, with the variability around these median projections increasing substantially through 2100 (Fig. 8). Simultaneously changing temperature and precipitation based on medians from all 24 climate projections also resulted in increases to streamflow, TDN, and TDP (Fig. 9). Specifically, ReNuMa predicted an approximate 6.0, 5.0, and 15.9% increase in streamflow, TDN, and TDP, respectively, by the year 2100 (Fig. 9a). ReNuMa output was relatively insensitive to changes in developed land; combining median climate projections for the year 2100 with a hypothetical 25% increase in developed land resulted in similar increases of 6.2, 5.1, and 15.7% in the same variables (Fig. 9b). Combining climate projections for the year 2100 with a hypothetical 25% increase in agricultural land resulted in a similar (6.8%) increase in streamflow, but much larger increases in loads of TDN (16.2%) and TDP (41.4%) (Fig. 9c).

DISCUSSION

Model Output: Calibration and Validation

The ReNuMa model has been applied to several watersheds in the northeastern United States and China (Hong and Swaney, 2013, Sha et al., 2013, Li et al., 2014, Sha et al., 2014). These watersheds range in size from ~400 km² to 70,000 km² and tend to have forested and agricultural land as the dominant two land cover types, often accounting for greater than 70% of the watershed (Hong and Swaney, 2013, Sha et al., 2013, Li et al., 2014, Sha et al., 2014). Mean annual temperature and precipitation for these watersheds range from 4.3 to 14.9 °C and 715 to 1700 mm y⁻¹, respectively. Additionally, the reported average elevations for some of these watersheds range between ~100 and 1500 m above mean sea level (Li et. 2014, Sha et al., 2014). ReNuMa has consistently captured a high percentage of the variance in observed discharge and nitrogen loads in these watersheds. Across the northeastern U.S. watersheds coefficients of variation for discharge and nitrogen loads were 0.83 and 0.90, respectively (Hong and Swaney 2013), while values in China were greater than 0.7 over the entire research period (Sha et al., 2013, Li et al., 2014, Sha et al., 2014). When compared to the watersheds where ReNuMa has been validated, the New River Estuary watershed has comparable characteristics in regards to size, land cover type and distribution, and precipitation patterns (Brush, 2013). As a result, it was hypothesized that the ReNuMa model would capture a significant portion of the variability in measured discharge and nutrient loading for the NRE watershed. Preliminary calibration of ReNuMa in several NRE subwatersheds using data from 2008 to 2011 further reinforced this hypothesis (Brush, 2013).

ReNuMa was a good predictor of streamflow, TDN load, and TDP load for the Gum Branch watershed as well as several MCBCL subwatersheds (Tables 4-6). Since the New River

is the dominant source of freshwater and allochthonous nutrients to the NRE, accurate model output was most critical for the watershed whose streamflow and dissolved nutrient loads enter into the New River which is Gum Branch. As hypothesized, the Gum Branch watershed displayed some of the highest coefficients of variation when examining regression plots of measured and modeled data. During the calibration phase, coefficients of variation were consistently greater than 0.6, ranged from ~0.4 to 0.6 during the validation period, and were consistently greater than 0.5 when examining the entire research period (Fig. 3). Such consistent results were expected since the characteristics of the Gum Branch watershed, such as size and land cover distribution, are comparable to other watersheds where ReNuMa has been successfully applied. Model output for most MCBCL subwatersheds was also classified as either good or intermediate, especially for discharge and TDN (Tables 4-6). These positive results were for subwatersheds with characteristics – particularly small size and low relief – that differed substantially from those where ReNuMa has been previously applied. Given the good to intermediate fits for Gum Branch and many of the MCBCL subwatersheds, ReNuMa is a useful tool for predicting loads to the NRE system.

Discrepancies in ReNuMa Model Output

Discrepancies between measured data and model output for some of the smaller watersheds on MCBCL may be reflective of watershed characteristics not typically associated with the systems where ReNuMa has been successfully applied such as watershed size, dominant land cover, and topography. The ability of any model to accurately simulate streamflow will be limited by how well precipitation patterns are captured within the watershed boundary. The precipitation data used in ReNuMa represented a spatial average of rain gauge stations within and slightly beyond the NRE watershed boundary. For the larger Gum Branch subwatershed,

these spatially averaged precipitation data appear to have reflected average precipitation conditions for the watershed as indicated by the good model output for streamflow, which in turn resulted in good model output for dissolved nutrients. The smaller subwatersheds on MCBCL, however, ranged in size from ~0.2 to 7.5 km², which may have inhibited good model estimates from ReNuMa. At such small spatial scales, catchment modeling requires knowledge of the spatial variability in precipitation at the same or smaller scale of the watershed boundary (Faures et al., 1995), since precipitation can be quite variable across short distances (Krajewski et al., 2003). This could have made the smaller subwatersheds on MCBCL more sensitive to the spatial precipitation average that was used across all subwatersheds.

While controlled predominantly by precipitation, streamflow exiting a watershed is also heavily influenced by dominant land cover (Petersen et al., 2017). Use of the SCS curve number approach to estimate runoff in ReNuMa assumes high curve number values for urban and wetland areas suggesting that most precipitation is directly converted to runoff (Hong and Swaney 2007). This assumption may explain in part the inability of ReNuMa to capture the variability in streamflow for some of the MCBCL subwatersheds. The dominant land covers for many of these subwatersheds are wetland and developed or urban areas, which often accounted for greater than 40% of each subwatershed. While the relationship between watershed urbanization and runoff is generally positive (Chen et al., 2017), the ability for all precipitation to be converted to runoff may be inhibited by vegetated areas interspersed with urbanized areas which may sequester a portion of the runoff. Additionally, the assumption that all precipitation is converted to runoff in wetland areas may not hold if the wetlands are characterized by hollows and hummocks that retain water until these ponded areas connect to the larger channel network and contribute to streamflow (Frei et al., 2010).

The relationship between watershed slope and runoff is often positively correlated (El-Hassanin et al., 1993). Excluding the influence of soil type, precipitation that falls on a steep surface has a greater chance of exiting the watershed as runoff because gravity affords it less time to be subjected to other watershed processes such as infiltration and transpiration, especially during very low precipitation events. All of the subwatersheds on MCBCL are relatively flat, which reduces the rate of runoff and increases the time for precipitation to be influenced by watershed processes before it can be incorporated into runoff. As a result, the relatively low relief of the subwatersheds located on MCBCL may also explain why ReNuMa was not as good a predictor of streamflow as in the Gum Branch subwatershed.

Regression analyses of coefficients of variation between measured and modeled streamflow and MCBCL watershed characteristics identified watershed slope as a primary driver of discrepancies between ReNuMa model output and measured data, explaining 65% of the variability in r^2 values for MCBCL subwatersheds (slope= 0.13, $p=0.015$) (Figure 10). Neither watershed size nor dominant land cover could explain the degree of fit between ReNuMa output and observations in the smaller watersheds. The insignificant relationships between r^2 and MCBCL watershed size and land cover do not negate that these characteristics may be impacting ReNuMa model output. Instead these results reinforce the complexity of watershed response to climatic forcing and suggest that a combination of these watershed characteristics may have caused ReNuMa model output to deviate substantially from measured values.

The relationships between modeled streamflow and modeled TDN and TDP loads were linear, with modeled streamflow explaining approximately 81% and 92% of the variability in modeled TDN and TDP loads, respectively. This indicates that the ability of ReNuMa to accurately model dissolved nutrient loads is highly dependent on the accuracy of predicted

streamflow. Consequently, watersheds in which model output was classified as good or intermediate for streamflow typically had good or intermediate output for dissolved nutrients, especially for TDN. Across all the subwatersheds in which ReNuMa was applied, model output was typically worse for TDP loads than for streamflow and TDN loads. Since the NRE is a nitrogen limited system however, it was more important to accurately model streamflow and subsequent TDN loads relative to TDP loads (Pearl et al.,2013). Still, the generally poorer fits for phosphorus are likely due to two assumptions ReNuMa makes when calculating dissolved phosphorus loads. The first of these assumptions is that all phosphates in normal septic tanks adsorb to and are retained in soil and thus do not contribute to TDP in streamflow (Hong and Swaney 2007). While there are many studies documenting how effective septic systems can be at removing a significant portion of phosphates from effluent before it reaches groundwater (Mechtensimer and Toor 2017), there is typically a portion of phosphorus that remains in dissolved form that contributes to TDP loads. ReNuMa also assumes that all phosphorus within runoff from urban areas will be in particulate form as it is assumed to adsorb to material in these areas (Hong and Swaney 2007). Again, this assumption does not hold true for all developed areas, and since developed area constituted 5-83% of the MCBCL subwatersheds, ReNuMa may not have accounted for a substantial portion of TDP from those areas. Additionally, model estimates for TDP loads do not incorporate phosphorus released from particulates upon entering the water column at low salinities (Hartzell and Jordan 2010) and could represent another possible reason for model underestimation of TDP loads.

Model Output: Climate and Land Use Scenarios

Climate Only

Incremental increases in temperature across the NRE watershed resulted in expected decreases in streamflow, TDN loads, and TDP loads, with a decrease of 6-10% by the year 2100. The inverse relationship between soil moisture and temperature offers one possible explanation for this response (Lakshmi et al., 2003). That is, decreased streamflow and nutrient loads resulting from increased temperature may be attributed to decreased soil moisture within the watershed, which may act to increase the amount of water that can be stored within the watershed as opposed to being carried off by runoff. Additionally, increased temperatures act to increase evapotranspiration, which may decrease the amount of water and associated nutrients lost via runoff. The observed impact of temperature on modeled runoff does not incorporate any potential effects that changes in temperature may have on precipitation, and consequently ReNuMa results do not agree well with the results of other studies examining the relationship between air temperature and runoff. When the relationship between increased air temperatures and runoff is examined on a global scale, the relationship between the two is often linear (Probst and Tardy 1989, Labat et al., 2004). This linear relationship is suggested to be a result of increased evaporation over the oceans coupled to increased continental precipitation or decreased continental evaporation, both of which would increase continental runoff (Labat et al., 2004).

Decreased precipitation across the NRE watershed resulted in anticipated decreases in streamflow, TDN loads, and TDP loads, while increased precipitation resulted in anticipated increases in these variables. As hypothesized, changes to runoff were much more sensitive to changing precipitation than temperature, resulting in a 20-50% increase in runoff with a 20% increase in precipitation. This is a result of the direct relationship between the amount of water entering a watershed via precipitation and the amount of water available to leave the watershed. This relationship is also influenced by the land use distribution within the NRE watershed. Soils

within agricultural and other vegetated areas within the NRE are often classified as having moderate-low infiltration rates based on the Natural Resources Conservation Service hydrologic soil group classification. As a result, increased precipitation may have increased soil saturation and thus increased runoff from these soils. For areas within the NRE watershed that were mostly urban, increased precipitation on urban surfaces are much more easily transported to adjoining water bodies as there is very little opportunity for infiltration; the relationship between urban land use and runoff has been documented in many watersheds (Jennings and Jarnagin 2001). Additionally, increased precipitation on wetland areas will increase the availability for ponded waters to connect and contribute to streamflow (Frei et al., 2010). As noted above, modeled TDN and TDP loads were strongly correlated with modeled streamflow. As a result, increasing the amount of precipitation entering the watershed should also increase the quantity of dissolved constituents exiting the watershed; this explains the increases in dissolved loads predicted by ReNuMa.

Land Use Only

The most likely changes to NRE watershed land cover would be conversion of naturally vegetated land to agricultural and developed areas representing the typical sequence of land use change resulting from human activity (Foley et al., 2005). Increasing agricultural land had a more pronounced impact on dissolved nutrient loads than streamflow; modeled streamflow increased by less than 2% under increased agricultural land cover while TDN and TDP loads increased by 23% and 50%, respectively. The differential responses of streamflow and dissolved nutrient loads can be attributed to the application of fertilizer which serves as an additional source of dissolved nutrients to streamflow. ReNuMa model results also indicate that agricultural land use will have a greater impact on loads of dissolved phosphorus relative to dissolved

nitrogen. This is likely due to the fact that dissolved nitrogen has several point and non-point sources from the watershed while the dominant source of dissolved phosphorus from the watershed is agricultural land.

Increasing developed land within the NRE watershed impacted streamflow and TDN loads as expected; streamflow increased as a result of less infiltration capacity associated with developed areas and TDN loads mirrored this output since they are directly related to streamflow. The relatively small increases (<1%) in streamflow and TDN reflect the way in which developed land was changed in the scenarios. Since developed land constitutes an already small percentage of the watershed (14.3%), increasing developed land by 10, 25, and 50% did not result in a large overall increase in developed land and as a result would have minimal impacts on resulting freshwater flow and dissolved loads. Surprisingly, TDP loads did not increase when developed land increased but instead decreased. Such decreases in loads can be attributed to the assumption made by ReNuMa about the behavior of phosphorus exiting urban areas. That is, most of the dissolved phosphorus exiting urban areas is assumed to bind to particles and exit the watershed in particulate form. As a result, while increasing developed land would increase loads of total phosphorus, that increase would be represented in particulate form. This assumption is not always representative of watershed systems and represents an area where ReNuMa model output could be misleading if solely relying on dissolved loads.

Cumulative Impacts of Climate and Land Use

Examining the individual impacts of climate and land use on streamflow and dissolved nutrient loads from the NRE watershed allowed for easier interpretation of cumulative impacts. When projected changes in temperature and precipitation act on the NRE watershed simultaneously, the model predicted a net increase in streamflow and dissolved loads through the

year 2100. As anticipated, this net increase represents the dominant impact of precipitation on resulting loads over temperature and agrees well with findings that suggest that precipitation as opposed to temperature has the greater impact on resulting loads (Karl and Riebsame 1989). Superimposing hypothetical increases to developed or agricultural land on top of projected changes in climate further amplified increases in modeled streamflow and nutrient loads for reasons identified above. This amplification in loads was more pronounced under increased agricultural land than developed land and may provide some insight for best management practices for the NRE in the face of climate change. Specifically, if both temperature and precipitation increase in the NRE as projected, maintaining nutrient loads at levels that do not degrade water quality will require continual examination and improvement of agricultural land management practices.

Implications for the NRE Ecology

Projected changes in streamflow and nutrient loading from the NRE watershed due to changes in climate and land use have the potential to substantially impact NRE ecology. Climatic variations impact the ecology of the NRE by first impacting riverine discharge which then influences flushing time, water column irradiance, nutrient input, and stratification (Peierls et al., 2012, Brush, 2013, Anderson et al., 2014). Under climate projections through the year 2100, ReNuMa predicts that both freshwater inputs and nutrient loads to the NRE will increase. Such increases are likely to decrease flushing time which may cause elevated nutrient concentrations, specifically nitrate, to be regularly observed further down estuary as opposed to the current location of maximum concentrations at the head of the estuary prior to phytoplankton uptake. Similarly, maximum concentrations of sediment and other particulates are also likely to be located further down estuary under decreased flushing times which would subsequently decrease

water column irradiance in this region. This spatial shift in maximum nitrate and particulate matter concentrations should also shift maximum chlorophyll-a concentrations further down estuary where algae are not light limited by particulates but still have adequate nutrients for growth.

Anthropogenically-induced increases and shifts in phytoplankton and particulate matter further down estuary may impact organisms of all trophic levels in the NRE. This is because such shifts will affect benthic-pelagic coupling in the water column and likely change the trophic state of the NRE. A shift in the maximum concentration of particulate matter combined with increased phytoplankton biomass further down estuary will increase light attenuation in the middle estuary region. The benthic microalgae filter, which removes approximately 28-64% and 45-70% of autochthonous nitrogen inputs in the summer and spring, respectively (Anderson et al., 2013), would be less effective at removing nutrients from the water column due to light limitation, which could potentially cause the middle estuary to be more susceptible to eutrophication and hypoxic bottom water. Potential eutrophic and hypoxic conditions in the NRE will be further amplified by the inability of benthic organisms found in the NRE such as suspension and deposit feeders to aid in the clearing of phytoplankton biomass (Brush, 2013).

Projected changes in streamflow and nutrient loads may have variable impacts on the ecosystem metabolism of the NRE. Increased stratification resulting from increases to freshwater inflow could enhance autotrophy in the NRE as stratification keeps phytoplankton more tightly coupled with watershed-derived nutrients at the water column surface. Increased freshwater flow will also increase terrestrial organic matter input to the NRE which will increase respiration rates and likely result in increased heterotrophic conditions (Croswell et al., 2017). Since enhanced freshwater flow enhances conditions for both increased autotrophic and heterotrophic

conditions in the estuary, it is difficult to determine the likely metabolic state for the system, especially under projected climate changes for the system. However, it is likely that the NRE will remain near metabolic balance over an annual cycle under projected increases in precipitation and nutrient loads as was documented for the system during two years with contrasting amounts of precipitation (Crosswell et al., 2017).

Summary

The ReNuMa model proved to be a useful tool for estimating streamflow and dissolved nutrient loads from the NRE subwatersheds. As anticipated, ReNuMa captured a substantial portion of the observed variability in streamflow, TDN, and TDP loads for the largest Gum Branch subwatershed. Such model output resulted in good fit classifications for Gum Branch which was significant because the Gum Branch watershed serves as the major source of material loads to the NRE. While fit classifications for the MCBCL subwatersheds were much more varied than for Gum Branch, resulting mainly from variations in watershed slope, and to a lesser degree dominant land cover and watershed size, ReNuMa for the most part also displayed predominately good to intermediate model fits across these subwatersheds. The relatively good model output across the NRE subwatersheds during the calibration and validation phase demonstrates the applicability of ReNuMa in this system.

When scaled to the entire system, ReNuMa confirmed that the upland, off-base watershed contributes the majority of freshwater inputs and dissolved nutrient loads to the NRE. Projected changes in climate were predicted to increase streamflow, TDN, and TDP loads by the year 2100, with projected changes in precipitation dominating over projected increases in temperature. These increases became further amplified under hypothetical increases in developed and especially agricultural land cover. The implications of these anticipated

alterations to streamflow and dissolved loads include potential increases in concentrations and changes in spatial distributions of parameters such as nutrient and chlorophyll-a maxima within the NRE, which may then affect the trophic state of the estuary. Coupling the ReNuMa model to an existing estuarine simulation model of the NRE (Brush et al., 2018) will enhance our ability to determine how the ecology of the estuary is likely to respond to changes in land use and climate.

Tables

Table 1. Data sources used to adapt and calibrate the ReNuMa model to the NRE.

Data type	Data Description	Data processing
Weather	25 historical surface observation stations with daily measurements of precipitation (mm) and air temperature (max. and min., °C) across eastern NC	Averaged daily data across stations; results provided by R. Boyles and A. Wootten, NCSU; min/max temperatures averaged
DEM	Digital elevation model	Calculated slope length and percent slope for each land use type to arrive at values for USLE parameters.
Land use/ Soil Type	National Land Cover Dataset (2006 and 2011) (NLCD) National Resources Conservation Service SSURGO soil data for Onslow County	Aggregated 15 land use types down to the 8 land use types required for ReNuMa Extracted <i>K</i> and hydrologic soil group data to use for USLE and Curve Number parameter values
Hydrology	10 monitoring stations with daily flow ($m^3 s^{-1}$) from 2009-2015, provided by M. Piehler, UNC; 1 USGS gauge station with daily flow data from 2008-2015	Aggregated daily flow to monthly sum for calibration and validation
Water quality	10 monitoring stations with monthly TN (mol), TP (mol) and sediment (kg) loads from 2009-2015, provided by M. Piehler, UNC; 1 USGS gauge station with concentrations measured by S. Ensign, DCERP, and loads estimated by M. Brush, VIMS.	--
Point Sources	E.P.A. Water Discharge Permits website (EPA-PCS 2009)	Divided the annual discharges by 12 to obtain monthly point source discharge rate
Population	Population census of 2010 Sewer service area shapefile	Merged to differentiate population on sewer versus septic
Atmospheric N deposition	Wet deposition from the National Atmospheric Deposition Program and dry deposition from EPA CastNet	Aggregated dry and wet deposition to total nitrogen deposition
*Data were collected through 2011 for 5 stations and through 2015 for the remaining 6 stations		

Table 2. Hydrologic parameters used in ReNuMa to estimate streamflow and sediment yield.

ReNuMa Hydrologic Parameters	Parameter Definition	Units	Range*	Source
Recession Coefficient	The rate at which streamflow returns to base flow after a storm f(streamflow)	d ⁻¹	0.2-0.9	Calculated
Seepage Coefficient	The rate at which groundwater in the shallow saturated zone of the aquifer seeps into the deep aquifer	d ⁻¹	0-1	ReNuMa autocalibration
Sediment Delivery Ratio	The ratio between the amount of sediment entering a watershed and the amount of sediment lost to erosion f(watershed area)	--	0.37-0.6	Calculated
Initial Saturation Conditions	Initial saturation conditions of the watershed subsurface	cm	0	ReNuMa Spin-up
Antecedent Moisture	Moisture (rain+snow melt) in the aquifer before the simulation period begins	cm	0	ReNuMa Spin-up
Unsaturated Storage Water Capacity	The amount of water the unsaturated zone of the aquifer is capable of holding	cm	10	ReNuMa default
Erosivity Coefficients	Coefficient used to estimate the amount of sediment lost from the watershed during rainfall events	--	0.16 (Cool Season) 0.28 (Warm Season)	Literature
Evapotranspiration Cover	Coefficient used to estimate the quantity of water lost during evaporation and transpiration f(land use, temperature)	--	0.8-1.0	Literature and Calculated
Runoff Curve Number	Number used to predict direct runoff following a rainfall event f(land use and soil type)	cm	53.5-100	Literature and Calculated
USLE Parameters	Parameters used for estimating annual soil loss due to erosion including: <i>K</i> = soil erodibility factor <i>LS</i> = topographic factor <i>C</i> = cover management factor <i>P</i> = supporting practice factor	mg•ha ⁻¹ y ⁻¹	0-0.48	Literature and Calculated

Table 3. Nutrient parameters used in ReNuMa to estimate nitrogen and phosphorus fluxes.

ReNuMa Nutrient Parameters	Parameter Definition	Units	Range*	Source
Nitrogen in Sediment	The amount of nitrogen present in soils of rural land covers	mg kg ⁻¹	1400	Literature
Phosphorus in Sediment	The amount of phosphorus present in soils of rural land covers	mg kg ⁻¹	352	Literature
Groundwater Nitrogen Concentration	The concentration of nitrogen in groundwater	mg l ⁻¹	1.1	Literature
Groundwater Phosphorus Concentration	The concentration of phosphorus in groundwater	mg l ⁻¹	0.013	Literature
Groundwater Denitrification Fraction	The fraction of groundwater nitrogen lost during denitrification	--	0.387	Literature
Per capita tank N effluent	Per capita daily nitrogen load in septic tank effluent	g d ⁻¹	13.2	Literature
Per capita tank P effluent	Per capita daily phosphorus load in septic tank effluent	g d ⁻¹	0.93	Literature
Per capita grow season N uptake	Per capita daily nitrogen uptake by plants	g d ⁻¹	1.6	Literature
Per capita grow season P uptake	Per capita daily phosphorus uptake by plants	g d ⁻¹	0.4	Literature
*Represents the range of values determined for the 11 subwatersheds in which ReNuMa was applied				

Table 4. Regression statistics between Measured and Modeled Streamflow for NRE subwatersheds

Watershed	Slope (Streamflow)	Intercept (Streamflow)	r^2 (Streamflow)	P (Streamflow)		
				Slope	Intercept	OMF*
1. Airport	0.19	23.32	0.07	<<0.001	0.015	0.13
2. Camp Johnson	0.52	-0.08	0.17	0.024	0.97	0.016
3. Cogdel	0.94	1.27	0.26	0.73	0.19	<<0.001
4. Courthouse	0.27	4.19	0.24	<<0.001	<<0.001	<<0.001
5. Freeman	1.23	-1.45	0.45	0.38	0.23	<<0.001
6. French	0.88	0.95	0.13	0.87	0.22	<<0.001
7. Gillets	1.14	-1.7	0.49	0.51	0.12	<<0.001
8. Gum Branch	0.9	-0.12	0.53	0.27	0.79	<<0.001
9. Southwest	0.16	3.55	0.08	<<0.001	0.016	0.09
10. Tarawa	0.73	0.41	0.08	0.35	0.61	0.013
11. Traps	0.63	1.72	0.58	<<0.001	<<0.001	<<0.001

Table 5. Regression statistics between Measured and Modeled TDN loads for NRE subwatersheds

Watershed	Slope (TDN)	Intercept (TDN)	r^2 (TDN)	P (TDN)		
				Slope	Intercept	OMF
1. Airport	0.15	0.04	0.06	<<0.001	0.01	0.18
2. Camp Johnson	0.40	-6.8e-04	0.19	<<0.001	0.55	0.013
3. Cogdels	1.12	0.02	0.28	0.56	0.34	<<0.001
4. Courthouse	0	0.09	0.21	<<0.001	0.0013	<<0.001
5. Freeman	0.79	-0.02	0.45	0.22	0.33	<<0.001
6. French	0.73	0.03	0.1	0.29	0.17	0.0043
7. Gillets	0.59	-0.02	0.46	0.001	0.21	<<0.001
8. Gum Branch	1.1	-1.65	0.53	0.38	0.50	<<0.001
9. Southwest	0.1	0.01	0.08	<<0.001	0.026	0.085
10. Tarawa	0.54	0.002	0.09	0.022	0.57	0.008
11. Traps	0.36	0.001	0.51	<<0.001	0.017	<<0.001

Table 6. Regression statistics between Measured and Modeled TDP loads for NRE subwatersheds

Watershed	Slope (TDP)	Intercept (TDP)	r^2 (TDP)	P (TDP)		
				Slope	Intercept	OMF
1. Airport	0.05	0.002	0.004	<<0.001	<<0.001	0.71
2. Camp Johnson	0.65	-1.6e-05	0.44	0.01	0.63	<<0.001
3. Cogdel	1.23	0.0019	0.26	0.32	0.001	<<0.001
4. Courthouse	1.9e-04	0.24	0.21	<<0.001	<<0.001	<<0.001
5. Freeman	1.13	-4.1e-04	0.63	0.44	0.24	<<0.001
6. French	0.44	0.001	0.11	<<0.001	<<0.001	0.003
7. Gillets	-0.0003	0.001	1.7e-06	<<0.001	<<0.001	0.99
8. Gum Branch	0.48	-0.04	0.54	<<0.001	0.65	<<0.001
9. Southwest	0.07	2.9e-04	0.06	<<0.001	<<0.001	0.14
10. Tarawa	0.14	1.02e-04	0.16	<<0.001	<<0.001	0.00017
11. Traps	1.33	1.01e-04	0.48	0.037	<<0.001	<<0.001

Figures

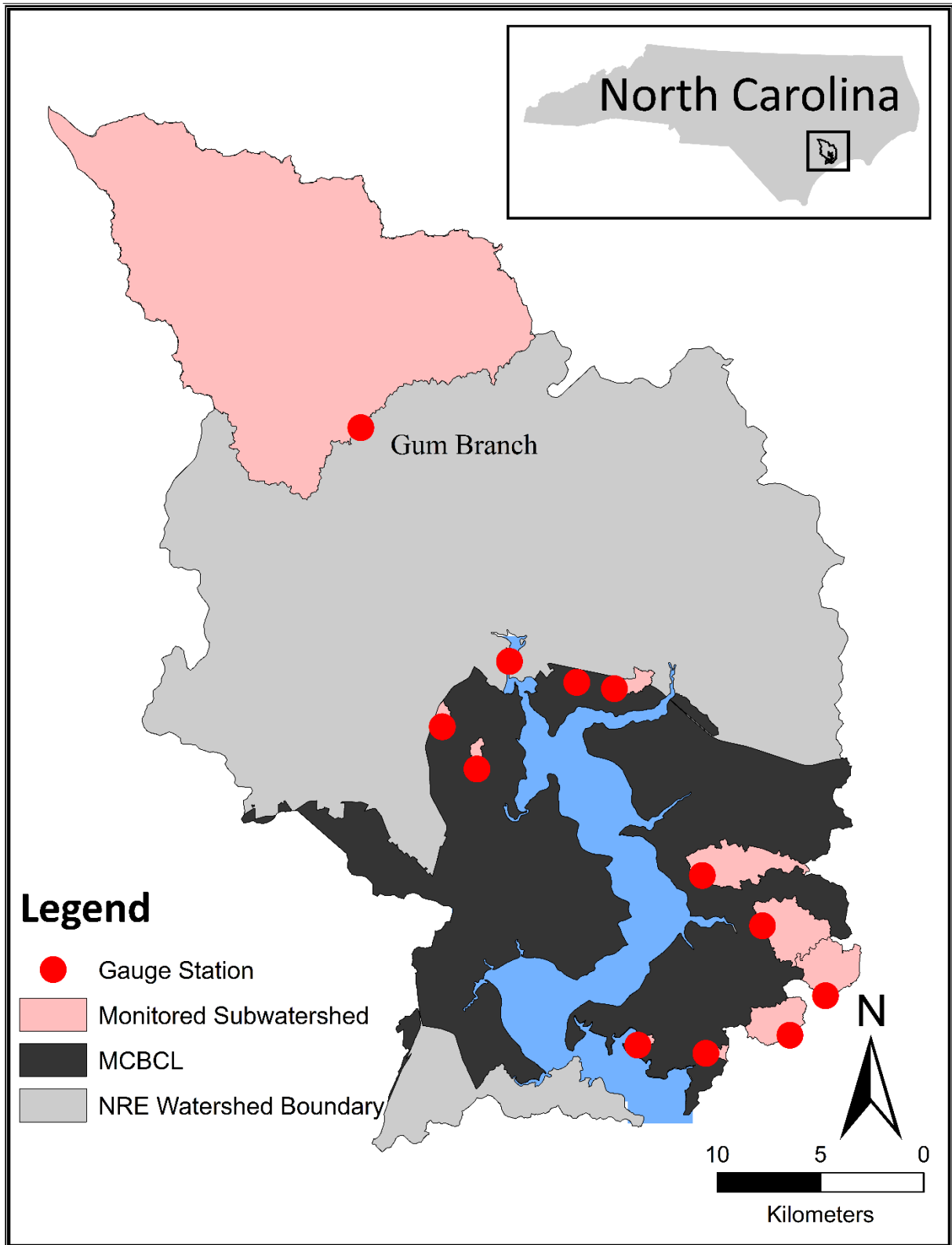


Figure 1. Location and watershed boundary of the NRE in North Carolina, MCBCL, gauging stations, and associated subwatersheds used during model calibration and validation.

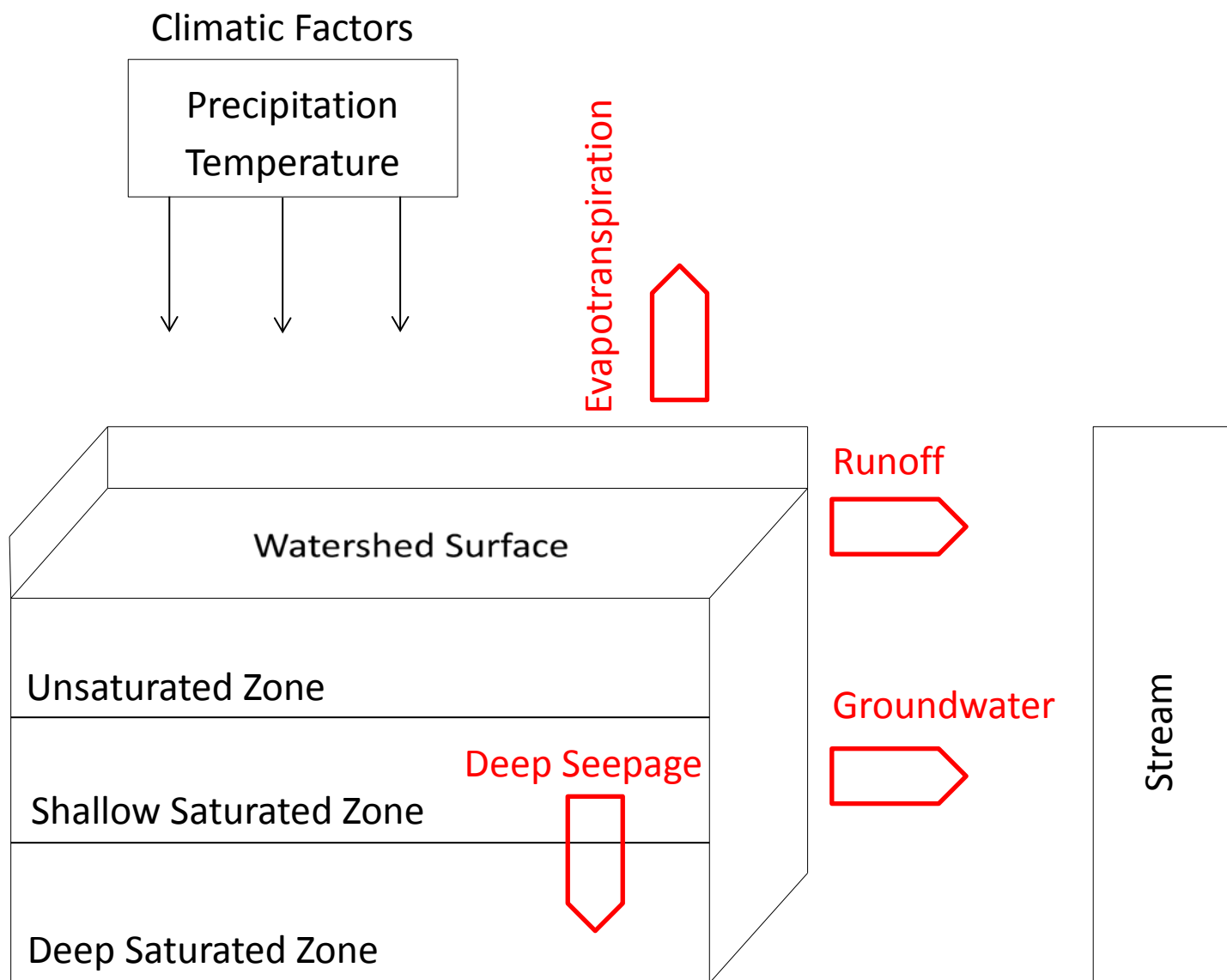


Figure 2a. Schematic of hydrological dynamics of the ReNuMa model (modified from Hong and Swaney 2007).

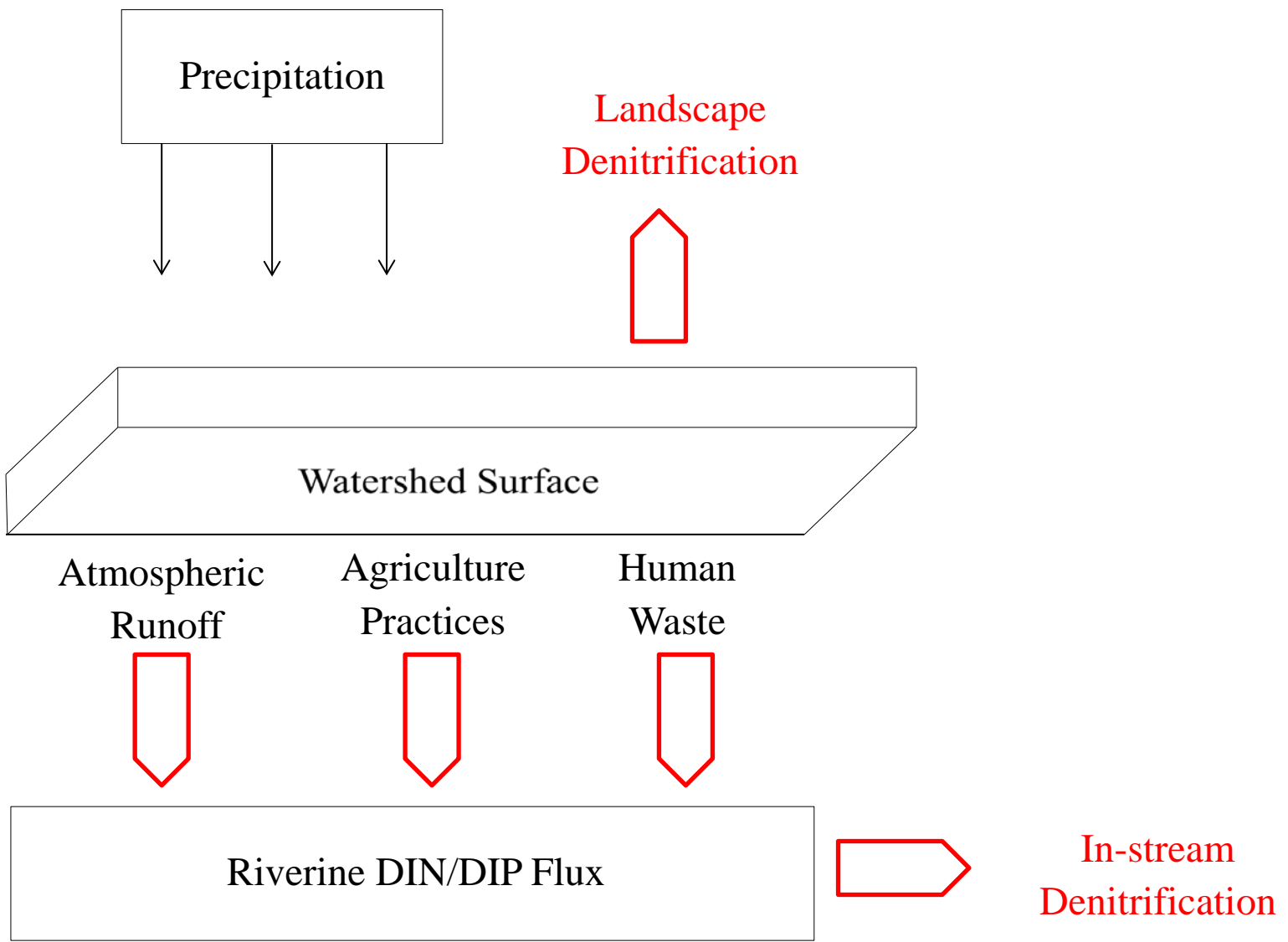


Figure 2b. Schematic of nutrient dynamics of the ReNuMa model (modified from Hong and Swaney 2007).

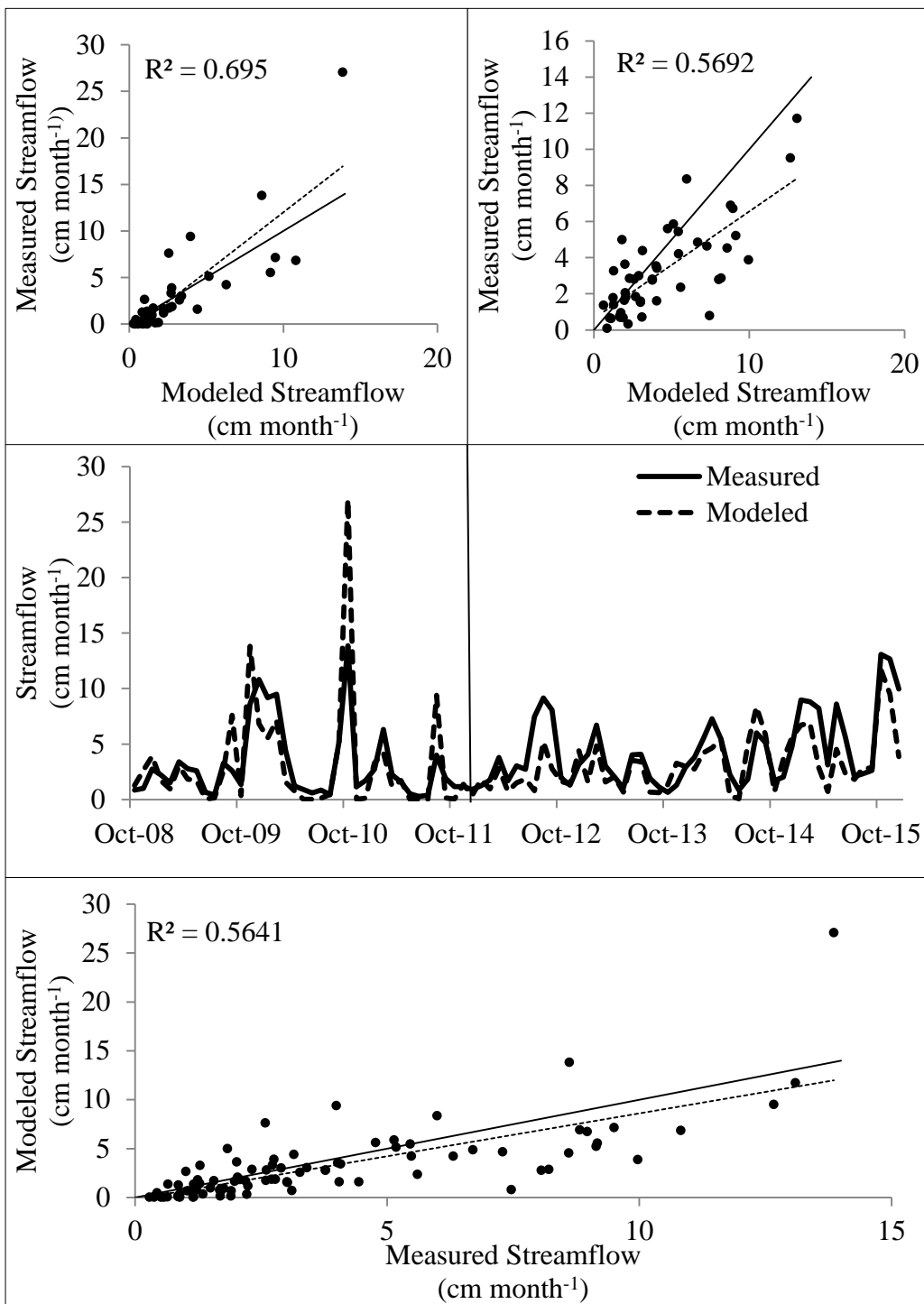


Figure 3. Measured and modeled streamflow for the Gum Branch subwatershed from 2008 to 2015. Top two regression plots display fits (dashed line) during the calibration (top left) and validation (top right) portion of the time series while bottom regression plot displays model fit (dashed line) over the entire time series. Solid line on regression plots is the 1:1 line. Streamflow is expressed as a yield (i.e., normalized to watershed area).

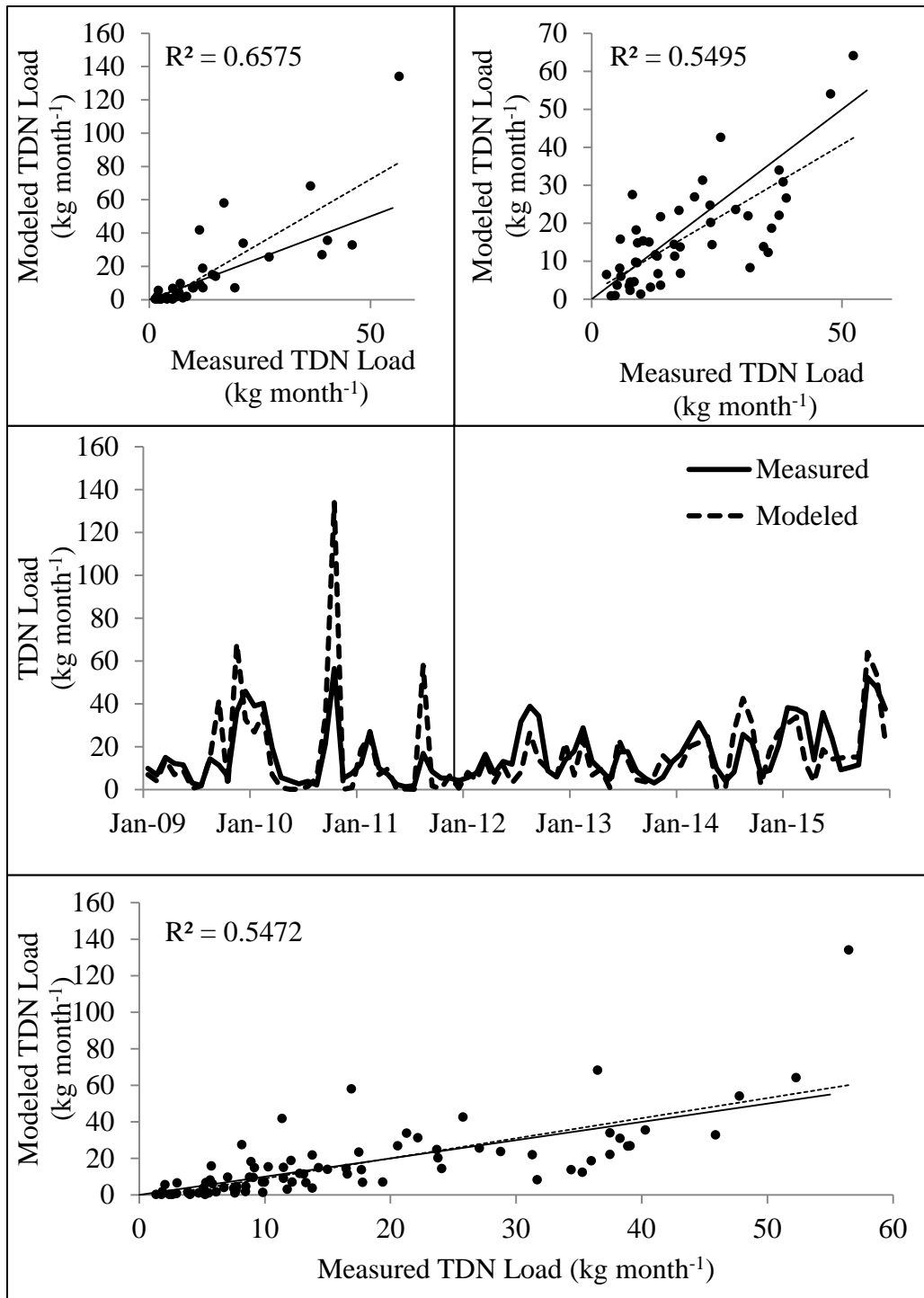


Figure 4. Measured and modeled TDN loading for the Gum Branch subwatershed from 2008 to 2015. Top two regression plots display fits (dashed line) during the calibration (top left) and validation (top right) portion of the time series while bottom regression plot displays model fit (dashed line) over the entire time series. Solid line on regression plots is the 1:1 line.

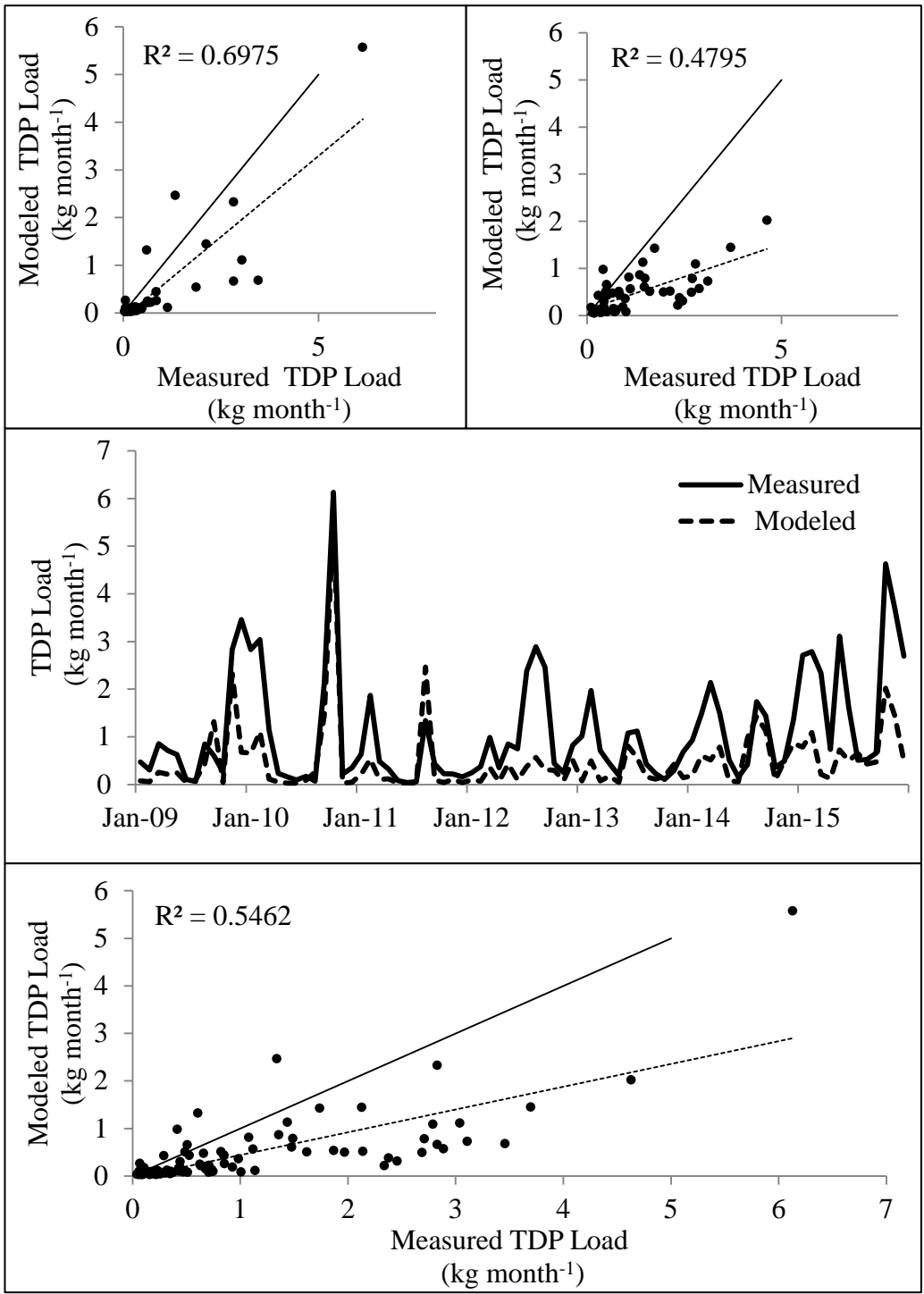


Figure 5. Measured and modeled TDP loading for the Gum Branch subwatershed from 2008 to 2015. Top two regression plots display fits (dashed line) during the calibration (top left) and validation (top right) portion of the time series while bottom regression plot displays model fit (dashed line) over the entire time series. Solid line on regression plots is the 1:1 line.

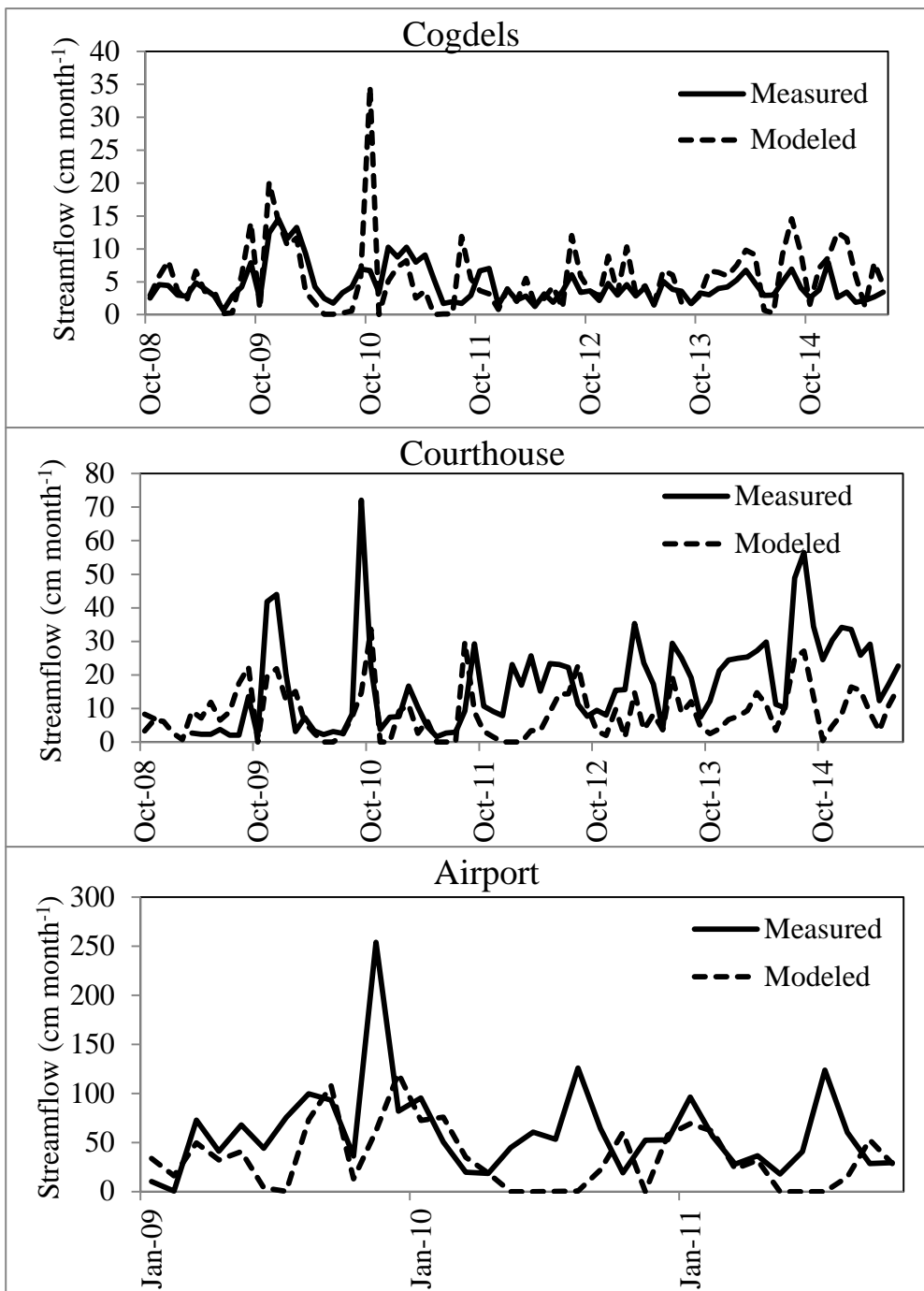


Figure 6. Example time series plots of streamflow for MCBCL subwatersheds representing good (Cogdel), intermediate (Courthouse), and poor (Airport) fit classifications. Streamflow is expressed as a yield.

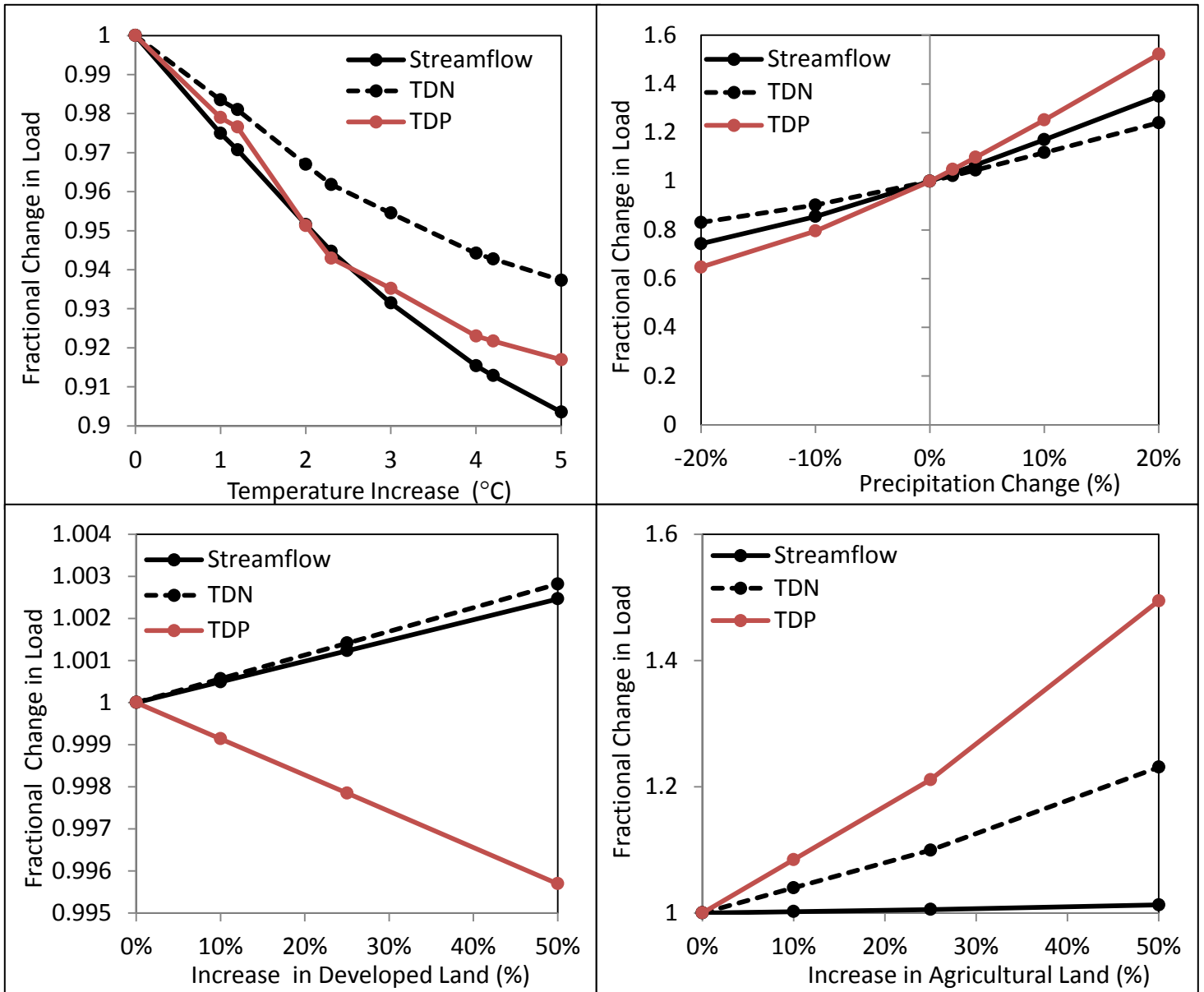


Figure 7. Fractional change in loads to the NRE under (a) increased temperatures, (b) changes in precipitation, (c) increased developed land (D) increased agricultural land.

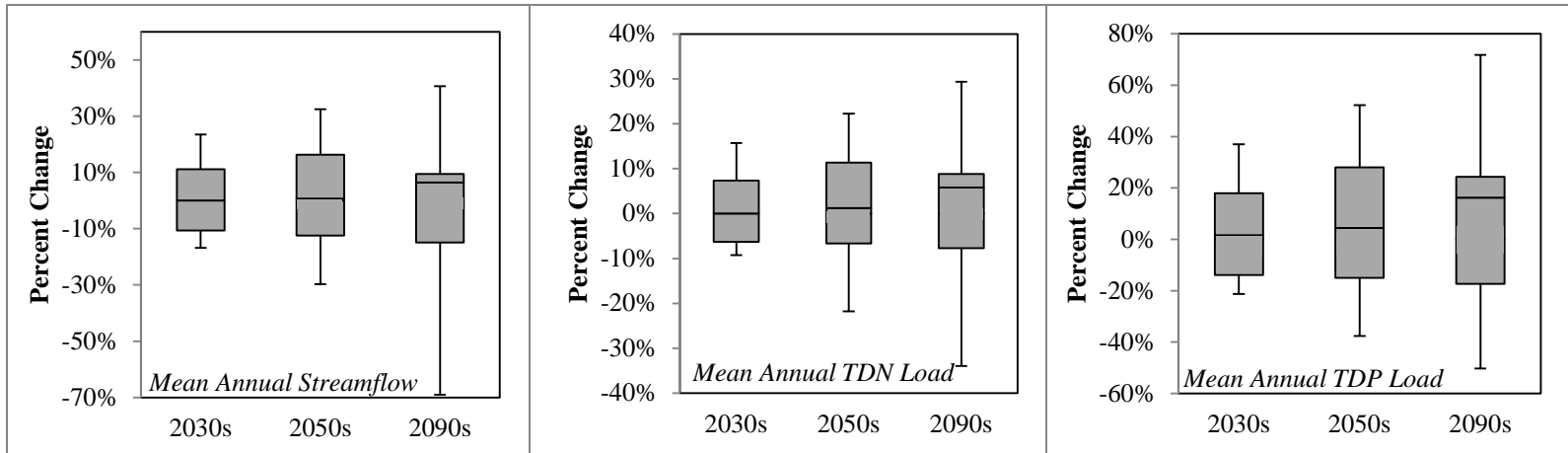


Figure 8. Box plots of modeled percent change in streamflow, TDN load, and TDP load for the NRE watershed based on 24 climate projections for the 2030s, 2050s, and 2090s. The solid line within the box denotes the median response from the 24 projections, boxes denote the 1st and 3rd quartiles, and error bars denote the minimum and maximum responses.

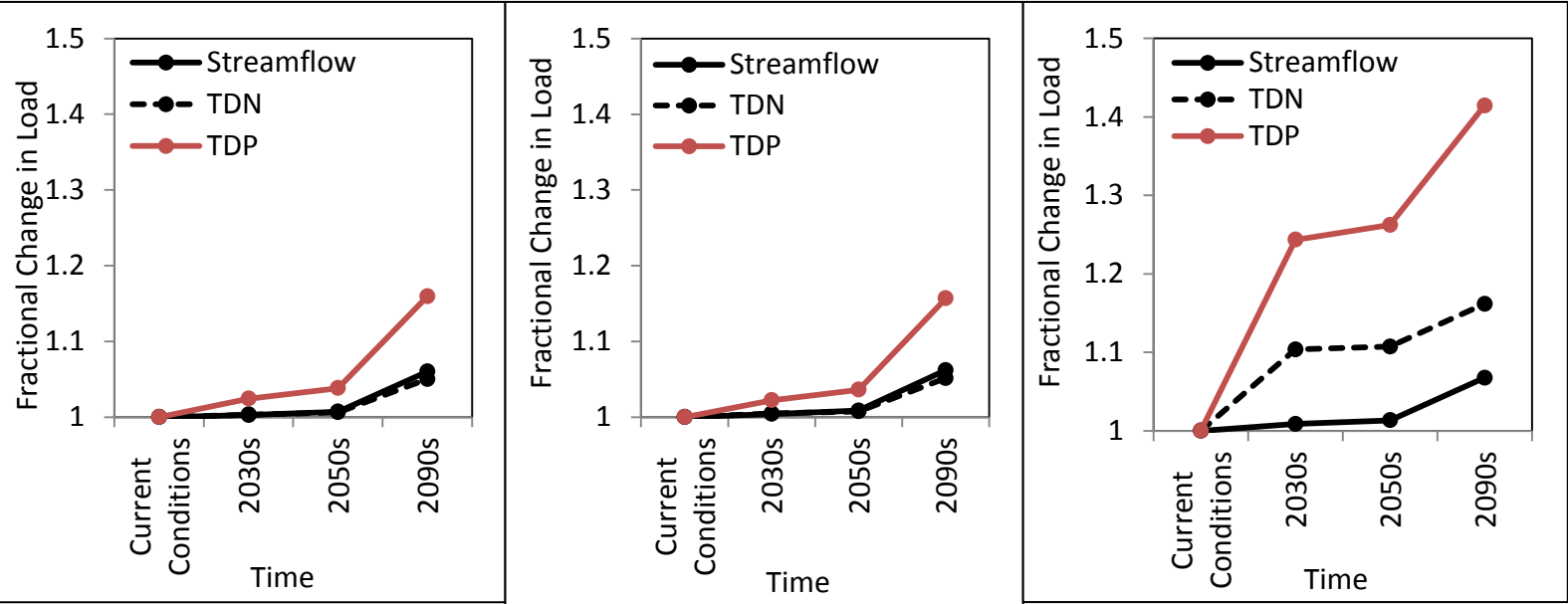


Figure 9. Fractional change in loads to the NRE under (a) decadal median climate projections for the NRE, (b) decadal median climate projections and a 25% increase in developed land, and (c) decadal median climate projections and a 25% increase in agricultural land. Median projected temperature increases for the NRE were 1.2, 2.3, and 4.2 °C for the 2030s, 2050s, and 2090s, respectively. Median projected precipitation increases for the NRE were 1.7%, 4.3%, and 9.6%, for the 2030s, 2050s, and 2090s, respectively.

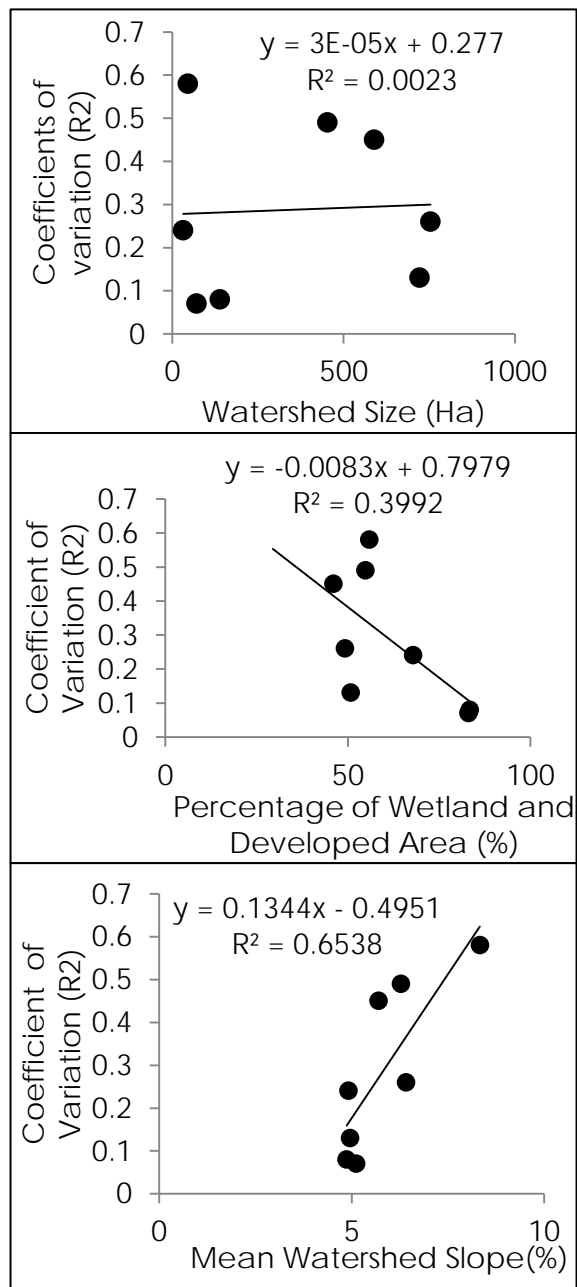


Figure 10. Coefficient of variation between measured and modeled streamflow as a function of MCBCL watershed characteristics (a) watershed size, (b) percentage of developed and wetland area, and (c) watershed slope obtained from Piehler et al. 2017.

Appendices

Appendix 1. Regression statistics between measured and modeled streamflow for NRE subwatersheds during calibration (2009-2011).

Watershed	Slope (Streamflow)	Intercept (Streamflow)	r^2 (Streamflow)	P (Streamflow)		
				Slope	Intercept	OMF*
1. Airport	0.19	23.32	0.07	<<0.001	0.015	0.13
2. Camp Johnson	0.52	-0.08	0.17	0.024	0.97	0.016
3. Cogdel	0.96	0.11	0.27	0.89	0.95	<<0.001
4. Courthouse	0.27	5.34	0.22	<<0.001	0.0027	0.0043
5. Freeman	1.23	-1.45	0.45	0.38	0.23	<<0.001
6. French	1.91	-0.05	0.21	0.15	0.97	0.0035
7. Gillet	1.14	-1.7	0.49	0.51	0.12	<<0.001
8. Gum Branch	1.36	-0.78	0.67	0.030	0.27	<<0.001
9. Southwest	0.16	3.55	0.08	<<0.001	0.016	0.09
10. Tarawa	0.76	0.76	0.05	0.66	0.60	0.16
11. Traps	0.61	1.39	0.58	<<0.001	0.039	<<0.001

Appendix 2. Regression statistics between measured and modeled streamflow for NRE subwatersheds during validation (2012-2015).

Watershed	Slope (Streamflow)	Intercept (Streamflow)	r^2 (Streamflow)	p (Streamflow)		
				Slope	Intercept	OMF*
1. Airport	--	--	--	--	--	--
2. Camp Johnson	--	--	--	--	--	--
3. Cogdel	1.62	-0.28	0.43	0.042	0.81	<<0.001
4. Courthouse	0.37	1.07	0.35	<<0.001	0.59	<<0.001
5. Freeman	--	--	--	--	--	--
6. French	0.69	0.97	0.21	0.14	0.13	0.0021
7. Gillet	--	--	--	--	--	--
8. Gum Branch	0.59	0.64	0.57	<<0.001	0.13	<<0.001
9. Southwest	--	--	--	--	--	--
10. Tarawa	0.77	-0.09	0.39	0.14	0.83	<<0.001
11. Traps	0.69	1.83	0.6	0.0011	<<0.001	<<0.001

Appendix 3. Regression statistics between measured and modeled TDN loading for NRE subwatersheds during calibration (2009-2011).

Watershed	Slope (TDN)	Intercept (TDN)	r^2 (TDN)	P (TDN)		
				Slope	Intercept	OMF*
1. Airport	0.15	0.04	0.06	<<0.001	0.01	0.18
2. Camp Johnson	0.40	-6.8e-04	0.19	<<0.001	0.55	0.013
3. Cogdel	1.15	-0.002	0.29	0.62	0.96	<<0.001
4. Courthouse	0.09	0.0035	0.22	<<0.001	0.0056	0.0041
5. Freeman	0.79	-0.02	0.45	0.22	0.33	<<0.001
6. French	1.61	0.01	0.18	0.28	0.84	0.0065
7. Gillets	0.59	-0.02	0.46	0.001	0.21	<<0.001
8. Gum Branch	1.56	-4.33	0.64	0.0088	0.27	<<0.001
9. Southwest	0.1	0.01	0.08	<<0.001	0.026	0.085
10. Tarawa	0.0033	0.60	0.07	0.27	0.56	0.11
11. Traps	0.37	1.0e-03	0.51	<<0.001	0.20	<<0.001

Appendix 4. Regression statistics between measured and modeled TDN loading for NRE subwatersheds during validation (2012-2015).

Watershed	Slope (TDN)	Intercept (TDN)	r^2 (TDN)	P (TDN)		
				Slope	Intercept	OMF*
1. Airport	--	--	--	--	--	--
2. Camp Johnson	--	--	--	--	--	--
3. Cogdel	1.73	-0.0042	0.43	0.025	0.86	<<0.001
4. Courthouse	0.11	0.0013	0.23	<<0.001	0.37	<<0.001
5. Freeman	--	--	--	--	--	--
6. French	0.46	0.03	0.18	0.001	0.0519	0.0049
7. Gillet	--	--	--	--	--	--
8. Gum Branch	0.78	1.79	0.55	0.040	0.45	<<0.001
9. Southwest	--	--	--	--	--	--
10. Tarawa	0.53	-6.9e-05	0.42	<<0.001	0.97	<<0.001
11. Traps	0.34	0.001	0.54	<<0.001	0.011	<<0.001

Appendix 5. Regression statistics between measured and modeled TDP loading for NRE subwatersheds during calibration (2009-2011).

Watershed	Slope (TDP)	Intercept (TDP)	r^2 (TDP)	P (TDP)		
				Slope	Intercept	OMF*
1. Airport	0.05	0.002	0.004	<<0.001	<<0.001	0.71
2. Camp Johnson	0.65	-1.6e-05	0.44	0.01	0.63	<<0.001
3. Cogdel	1.93	-0.00018	0.59	0.0012	0.80	<<0.001
4. Courthouse	0.2	0	0.11	<<0.001	<<0.001	0.047
5. Freeman	1.13	-4.1e-04	0.63	0.44	0.24	<<0.001
6. French	0.32	0.0014	0.09	<<0.001	<<0.001	0.068
7. Gillet	-0.0003	0.001	1.7e-06	<<0.001	<<0.001	0.99
8. Gum Branch	0.69	-0.11	0.7	<<0.001	0.40	<<0.001
9. Southwest	0.07	2.9e-04	0.06	<<0.001	<<0.001	0.14
10. Tarawa	0.16	9.9e-05	0.13	<<0.001	0.0055	0.024
11. Traps	1.27	8.3e-05	0.52	0.201	0.0064	<<0.001

Appendix 6. Regression statistics between measured and modeled TDP loading for NRE subwatersheds during validation (2012-2015).

Watershed	Slope (TDP)	Intercept (TDP)	r^2 (TDP)	P (TDP)		
				Slope	Intercept	OMF*
1. Airport	--	--	--	--	--	--
2. Camp Johnson	--	--	--	--	--	--
3. Cogdel	0.41	0.0039	0.03	0.11	<<0.001	0.25
4. Courthouse	0.28	1.6e-04	0.27	<<0.001	0.0086	<<0.001
5. Freeman	--	--	--	--	--	--
6. French	1.01	0.00051	0.21	0.97	0.35	0.0021
7. Gillet	--	--	--	--	--	--
8. Gum Branch	0.28	0.13	0.48	<<0.001	0.07	<<0.001
9. Southwest	--	--	--	--	--	--
10. Tarawa	0.13	1.02e-04	0.21	<<0.001	<<0.001	0.0024
11. Traps	1.41	1.15e-04	0.41	0.13	0.0015	<<0.001

Appendix 7. ReNuMa model skill assessment for streamflow from 11 NRE subwatersheds, showing absolute mean and median error (ABS Error), percent mean and median error (% Error), and root mean squared error (RMS Error), using model output over the entire time series. Units of ABS and RMS Error are cm month^{-1} .

Watershed	Absolute Error		% Error		RMSE
	Mean	Median	Mean	Median	
Airport	38.0	25.9	103.8	-27.3	54.7
Camp Johnson	6.59	5.34	-48.0	-74.8	8.50
Cogdel	2.99	2.20	27.2	5.8	4.69
Courthouse	10.9	7.88	-14.1	-55.8	14.3
Freeman	2.13	1.11	-47.3	-61.0	4.12
French	1.80	1.04	58.4	1.1	3.44
Gillet	2.24	1.36	-81.3	-54.2	3.87
Gum Branch	1.77	0.938	2.02	-36.0	3.45
Southwest	6.86	2.59	-10.4	-63.6	12.6
Tarawa	1.60	0.929	7.21	-49.1	3.50
Traps	2.30	1.40	1956.9	4.92	3.13

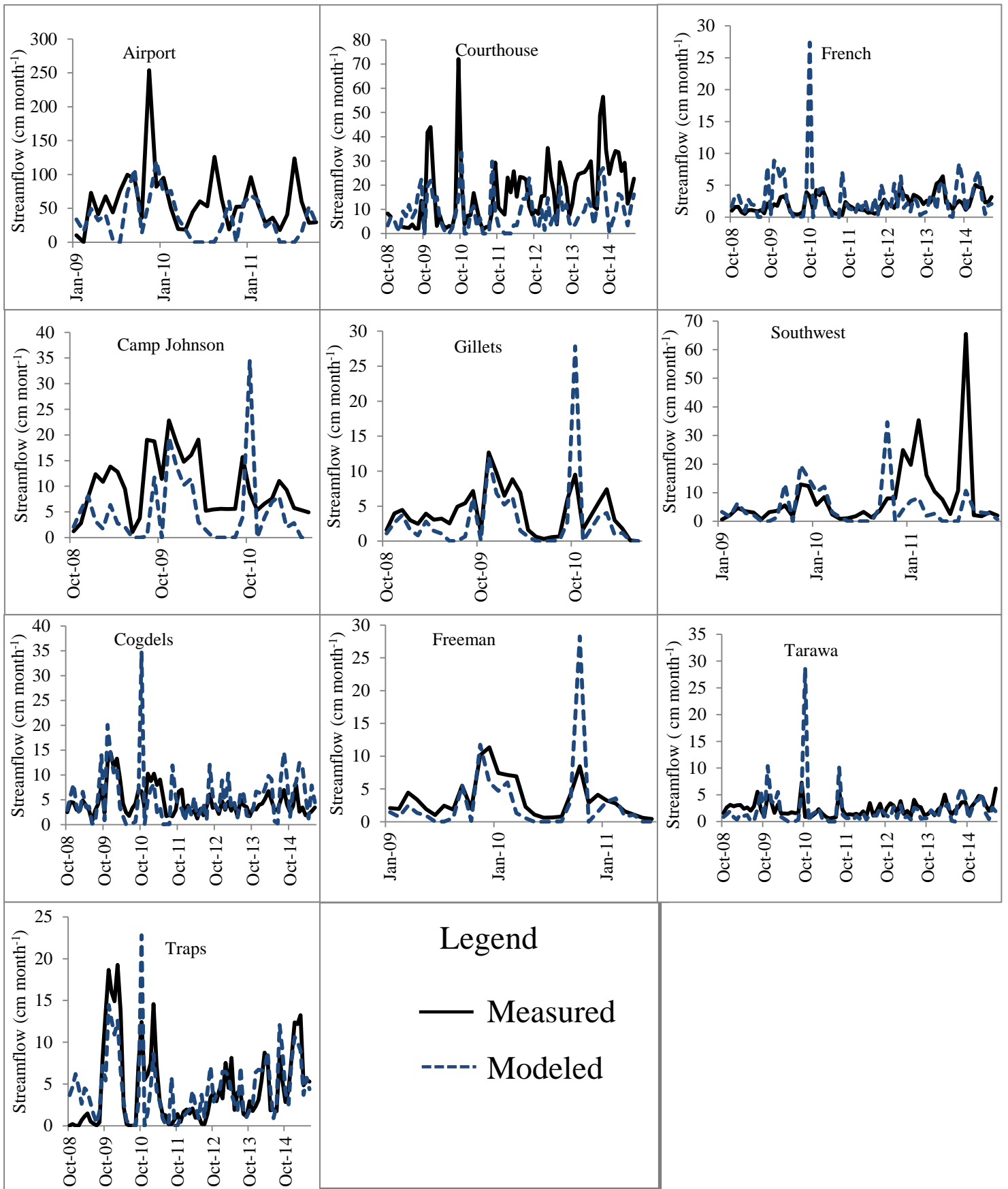
Appendix 8. ReNuMa model skill assessment for TDN loads from 11 NRE subwatersheds, showing absolute mean and median error (ABS Error), percent mean and median error (% Error), and root mean squared error (RMS Error), using model output over the entire time series. Units of ABS and RMS Error are kg month^{-1} .

Watershed	Absolute Error		% Error		RMSE
	Mean	Median	Mean	Median	
Airport	0.072	0.054	-25.8	-42.1	0.10
Camp Johnson	0.0050	0.0049	-70.6	-84.3	0.0057
Cogdel	0.068	0.052	91.5	68.6	0.11
Courthouse	0.026	0.020	80.3	85.1	0.035
Freeman	0.058	0.033	-64.6	-72.5	0.089
French	0.051	0.029	120.8	81.1	0.10
Gillet	0.068	0.052	-74.4	-74.9	0.087
Gum Branch	8.1	4.6	57.4	43.4	13.9
Southwest	0.016	0.0047	-47.0	-84.2	0.035
Tarawa	0.0088	0.0065	95.4	62.0	0.017
Traps	0.0050	0.0032	1297.1	68.0	0.0071

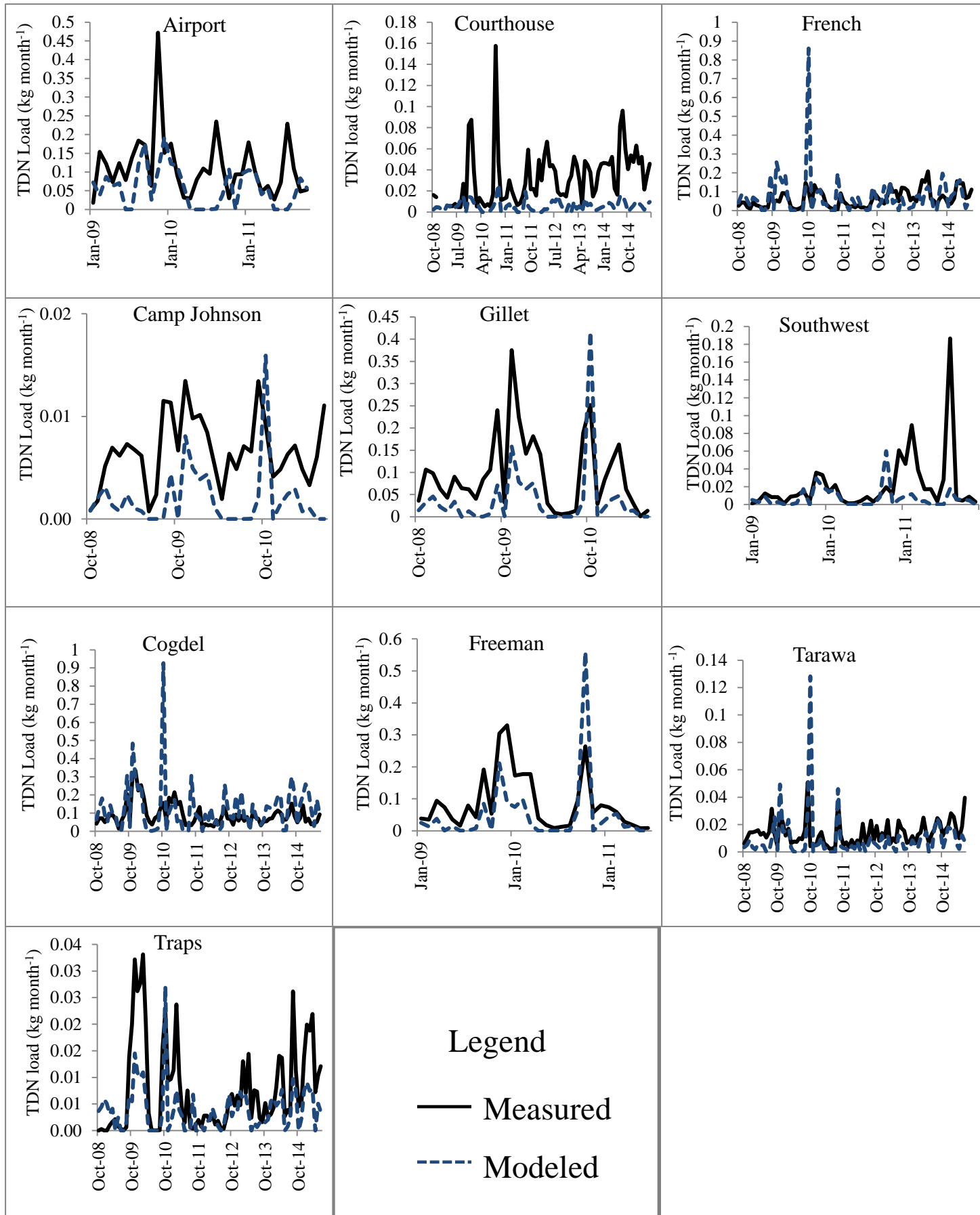
Appendix 9. ReNuMa model skill assessment for TDP loads for 11 NRE subwatersheds, showing absolute mean and median error (ABS Error), percent mean and median error (% Error), and root mean squared error (RMS Error), using model output over the entire time series.

Units of ABS and RMS Error are kg month^{-1} .

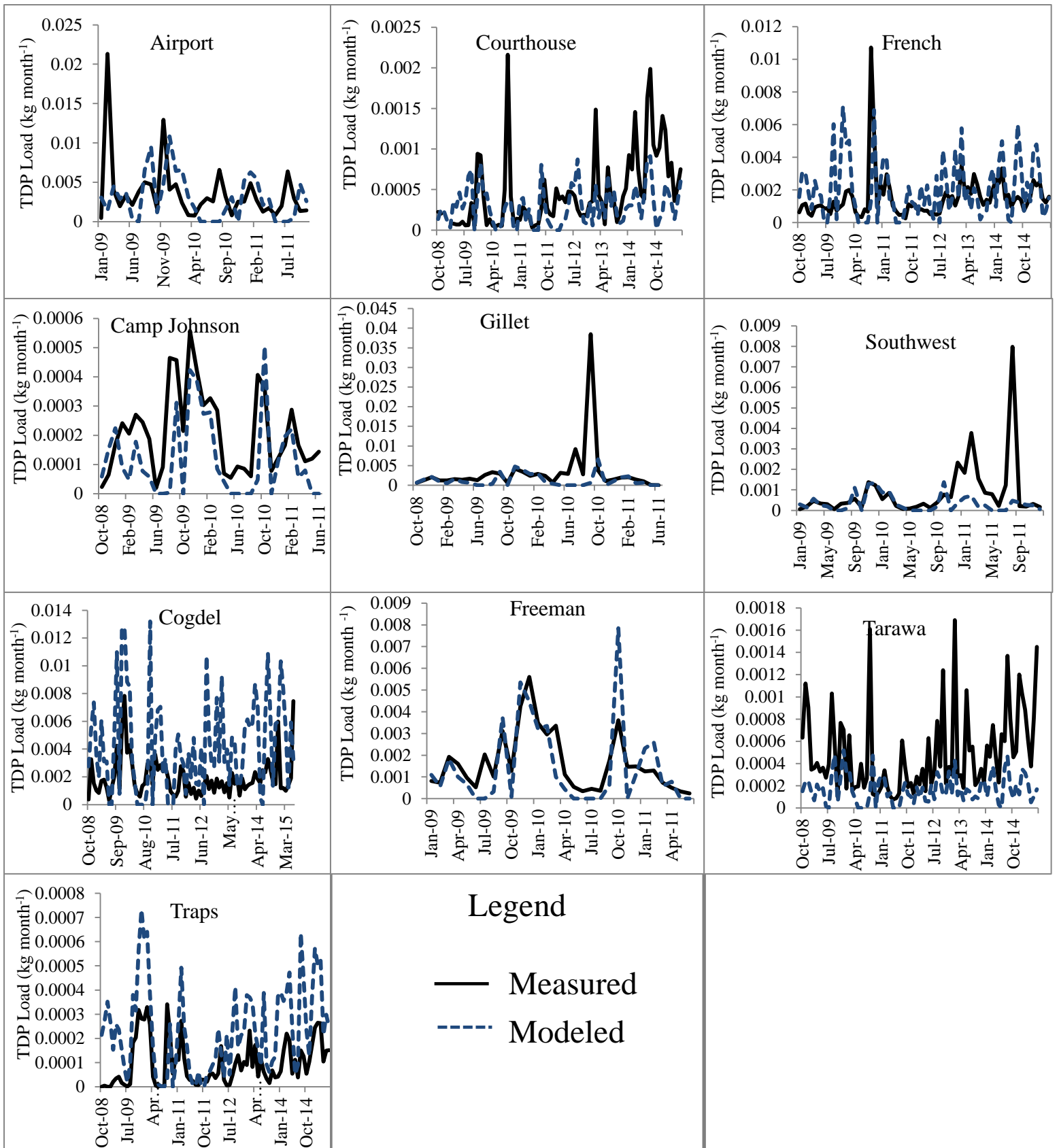
Watershed	Absolute Error		% Error		RMSE
	Mean	Median	Mean	Median	
Airport	0.0031	0.0023	35.3	19.9	0.0047
Camp Johnson	0.00011	0.000091	-43.73	-66.2	0.00015
Cogdel	0.0029	0.0022	187.7	140.0	0.0038
Courthouse	0.00030	0.00018	106.9	63.1	0.00043
Freeman	0.00082	0.00053	-32.5	-34.1	0.0012
French	0.0013	0.00087	105.5	87.4	0.0019
Gillet	0.0023	0.00053	-43.5	-50.0	0.0069
Gum Branch	0.68	0.39	66.4	67.0	1.0006
Southwest	0.00064	0.00019	-27.3	-64.7	0.0015
Tarawa	0.00034	0.00020	66.7	64.2	0.00046
Traps	0.00015	0.00013	4400.3	134.8	0.00019



Appendix 10. Time series plots of measured and modeled streamflow for all 10 MCBCL subwatersheds. Streamflow is expressed as a yield.



Appendix 11. Time series plots of measured and modeled TDN loading for all 10 MCBC subwatersheds



Appendix 12. Time series plots of measured and modeled TDP loading for all 10 MCBC subwatersheds.

LITERATURE REVIEW

- Alber, M. (2002) A conceptual Model of Estuarine Freshwater Inflow Management, *Estuaries*, 25(6B), 1246-1261.
- Alber, M. and Sheldon, J.E. (1999) Use of a Date-Specific Method to examine variability in Flushing times of Georgia Estuaries, *Estuarine, Coastal and Shelf Science*, 49, 469-482.
- Alexander, L.V., Zhnag, X., Peterson, T.C., Caesar, J., Gleason, B., Tank, A.M.,G, Haylock, M., Trewin,B., Rahimzadeh, Tagipour,A., Kumar, K.R., Revadekar, J., Griffiths, G., Vincent, L., Stephenson, D.B., Burn, J., Aguilar, E., Brunet, M., Taylor, M., Zhai, P., Rusticci, M., Vazquez-Aguirre, J.L. (2006) Global observed changes in daily climate extremes of temperature and precipitation, *Journal of Geophysical Research*, 111 (D5), 1-22.
- Alhajjar, B. J., J. M. Harkin, and G. Chesters(1989) Detergent Formula and Characteristics of Wastewater in On-site Tanks. *Journal of Water Pollution*. 61: 605-613.
- Anderson, D.M., Glibert, P.M., Burkholder, J.M. (2002) Harmful algal blooms and eutrophication: nutrient sources, composition and consequences, *Estuaries* 25, 562–584.
- Anderson, I.C., Brush, M.J., Piehler, M., Currin, C. (2013) Developing Indicators of Ecosystem Function for Shallow Estuaries: Benthic Functional Responses in the New River Estuary. Chapter 5 in: Final Technical Report to the Defense Coastal/Estuarine Research Program (DCERP1), RTI International, Research Triangle Park, NC.
- Anderson, I.C., Brush, M.J., Piehler, M.F., Currin, C.A., Stanhope, J.W., Smyth, A.R., Maxey, J.D., Whitehead, M.L. (2014) Impacts of Climate-Related Drivers on the Benthic Nutrient Filter in a ShallowPhotic Estuary, 37, S46-S62.
- Arnold Jr, C.L. and Gibbons, C.J. (1996) Impervious Surface Coverage: The Emergence of a Key Environmental Indicator, *Journal of the American Planning Association*, 62:2, 243-258, DOI: 10.1080/01944369608975688
- Baptista, J., Martinho, F., Dolbeth, M., Viegas, I., Cabral, H., and Pardal, M. (2010) Effects of freshwater flow on the fish assemblage of the Mondego estuary (Portugal): comparison between drought and non-drought years, *Marine and Freshwater Research*, 61(4), 490-501.
- Basnyat, P., Teeter, L.D., Flynn, K.M., Lockaby, B.G. (1999) Relationships between landscape characteristics and nonpoint source pollution inputs to coastal estuaries, *Environmental Management*, 23(4), 539-549.
- Bowen, J.L. and Valiela, I. (2001) The ecological effects of urbanization of coastal watersheds: historical increases in nitrogen loads and eutrophication of Waquoit Bay estuaries, *Can. J. Fish Aquat. Sci.*, 58, 1489-1500.
- Boyer, J.N., Christian, R.R., and Stanley, D.W. (1993). Pattern of Phytoplankton primary productivity in the Neuse River estuary, North Carolina, *Marine ecology Press Series*, 97, 287-297.
- Boynton, W R and W.&I Kemp(2000) Influence of river flow and nutrient loads on selected ecosystem processes: A synthesis of Chesapeake Bay Data, pp 169-298 In: J E Hobbie (Ed) *Estuarine Science –A Synthetic Approach to Research and Practice*, Island Press. Washington, DC.
- Brush, M.J. (2013) Development and Application of Watershed and Estuarine Simulation Models for the New River Estuary. Chapter 6 in: Final Technical Report to the Defense Coastal/Estuarine Research Program (DCERP1), RTI International, Research Triangle Park, NC.

- Brush, M.J. and L.A. Harris (2016) Ecological modeling. Pp. 214-223 in: Kennish, M.J. (ed.), Encyclopedia of Estuaries. Encyclopedia of Earth Sciences Series, Springer Netherlands
- Chanton, J. and Lewis, F.G. (2002) Examination of coupling between primary and secondary production in a river-dominated estuary: Apalachicola Bay, Florida, U.S.A., *Limnol. Oceanogr.*, 47(3), 683-697.
- Chen, J, Thellar, L., Gitau, MW, Engal, BA, Harbor, JM (2017) Urbanization impacts on surface runoff of the contiguous United States, *Journal of Environmental Management*, 187, 470-481.
- Cloern, J.E. (2001) Our evolving conceptual model of the coastal eutrophication problem, *Marine Ecology Progress Series*, 210, 223-253.
- Crosswell, J.R., Anderson, I.C., Stanhope, J.W., Dam, B.V., Brush, M.J., Ensign, S., Piehler, M.F., McKee, B., Bost, M., Pearl, H.W. (2017) Carbon budget of a shallow, lagoonal estuary: Transformations and source-sink dynamics along the river-estuary-ocean continuum, *Limnology and Oceanography*, 62, S29-S45.
- Doll, P. and Schmied, H.M. (2012) How is the impact of climate change on river flow regimes related to the impact on mean annual runoff? A global-scale analysis, *Environmental Research Letters*, 7(1), 1-11.
- Dore, M.H.I. (2005). Climate change and changes in global precipitation patterns: What do we know?, *Environment International*, 31, 1167-1181.
- Diaz, R.J. and Rosenberg, R. (2008) Spreading Deadzones and Consequences for Marine Ecosystems, *Science*, 321(5891), 926-929.
- Drewry, J.J., Newham, L.T.H., and Croke, B.F.W. (2009) Suspended sediment, nitrogen and phosphorus concentrations and exports during storm-events to the Tuross estuary, Australia, *Journal of Environmental Management*, 90(2), 879-887.
- El-Hassanin, A.S., Labib, T.M. , Gaber, E.I. (1993) Effect of vegetation cover and land slope on runoff and soil losses from the watersheds of Burundi, *Agriculture, Ecosystems and Environment*, 43 301-308.
- Ensign, S. (2017) AEM-4: New River. Chapter 4 in: Final Technical Report to the Defense Coastal/Estuarine Research Program 2 (DCERP2), RTI International, Research Triangle Park, NC.
- Ensign, S.H., Halls, J.N., and Mallin, M.A. (2004) Application of digital bathymetry data in an analysis of flushing times of two large estuaries, *Computers and Geosciences*, 30, 501-511.
- EPA (Environmental Protection Agency), (1999) Protocol for Developing Nutrient TMDLs. Report 841-B-99-007, Office of Water, U.S. Environmental Protection Agency, Washington, DC, 137
- Faures, J., Goodrich, D.C., Woolhiser, D.A., Sorooshian, S. (1995) Impact of small-scale spatial variability on runoff modeling, *Journal of Hydrology*, 173, 309-326.
- Foley, J.A., DeFries, R., Asner, G.P., Barford, C., Bonan, G., Carpenter, S.R., Chapin, F.S., Coe, M.T., Daily, G.C., Gibbs, H.K., Helkowski, J.H., Holloway, T., Howard, E.A., Kucharik, C.J., Monfreda, C., Patz, J.A., Prentice, I.C., Ramankutty, N., Snyder, P.K. (2005) Global Consequences of Land Use, *Science*, 309, 570-574.
- Frei, S., Lischeid, G., Fleckenstein, J.H. (2010) Effects of micro-topography on surface-subsurface exchange and runoff generation in a virtual riparian wetland-A modeling study, *Advances in Water Resources*, 33(11), 1388-1401.

- Fry, J., Xian, G., Jin, S., Dewitz, J., Homer, C., Yang, L., et al. (2011). Completion of the 2006 National Land Cover Database for the Conterminous United States. *Photogramm. Eng. Remote Sensing* 77, 858–864.
- Gordon, L., Dunlop, M., Foran, B. (2003) Land cover change and water vapour flows: learning from Australia, *Phil. Trans. R. Soc. Lond. B.*, 358, 1973-1984.
- Haith, D.A., R. Mandel, and R.S. Wu, (1992) Generalized Watershed Loading Functions Version 2.0 User's Manual, Cornell University, Ithaca, New York.
- Hall, N.S., Pearl, H.W., Peierls, B.L., Whipple, A.C. (2013) Effects of climatic variability on phytoplankton community structure and bloom development in the eutrophic, microtidal, New River Estuary, North Carolina, USA, *Estuarine, Coastal, and Shelf Science*, 117 (20), 70-82.
- Halliday, I.A., Robins, J.B., Mayer, D.G., Stauton-Smith, J. and Sellin, M.J. (2008) Effects of freshwater flow on the year-class strength of a non-diadromous estuarine finfish, king threadfin (*Polydactylus macrochir*), in a dry-tropical estuary, *Marine and Freshwater Research*, 59(1), 157-164.
- Hartzell, J.L. and Jordan, T.E. (2010) Shifts in the relative availability of phosphorus and nitrogen along estuarine salinity gradients, *Biogeochemistry*, 107, 489-500.
- Hickey, R. 2000. Slope Angle and Slope Length Solutions for GIS. *Cartography*, 29: 1 (1 – 8).
- Homer, C. G., Dewitz, J. A., Yang, L., Jin, S., Danielson, P., Xian, G., et al. (2015). Completion of the 2011 National Land Cover Database for the conterminous United States- Representing a decade of land cover change information. *Photogramm. Eng. Remote Sensing* 81, 345–354. doi: 10.14358/PERS.81.5.345
- Hong, B., and D. P. Swaney. (2007) Regional Nutrient Management (ReNuMa) Model, Version 1.0. User's Manual. Available at: <http://www.eeb.cornell.edu/biogeo/anc/usda/renuma.htm>. Then select: "Download <http://www.eeb.cornell.edu/biogeo/nanc/usda/renuma.htm>".
- Howarth, R.W., Fruci, J.R. and Sherman, D. (1991) Inputs of Sediment and Carbon to an estuarine ecosystem: Influence of Land Use, *Ecological Applications*, 1(1), 27-39.
- Huang, J., Li, Q., Tu, Z., Pan, C., Zhang, L., Ndokoye, P., Lin, J., Hong, H. (2013) Quantifying land-based pollutant loads into coastal area with sparse data: Methodology and application in China. *Ocean and Coastal Management*, 14-28.
- IPCC, 2007: Climate Change 2007: The Scientific Basis. Contribution of Working Group I to the Fourth Assessment Report of the Intergovernmental Panel on Climate Change, S. Solomon et al. (Eds.), Cambridge University Press, Cambridge and New York, 104pp
- IPCC (2013). Climate Change 2013: The Physical Science Basis. Contribution of Working Group I to the Fifth Assessment Report of the Intergovernmental Panel on Climate Change [Stocker, T.F., D. Qin, G.-K. Plattner, M. Tignor, S.K. Allen, J. Boschung, A. Nauels, Y. Xia, V. Bex and P.M. Midgley (eds.)]. Cambridge University Press, Cambridge, United Kingdom and New York, NY, USA.
- Jennigs, D.B. and Jarnagin, S.T. (2001) Changes in anthropogenic impervious surfaces, precipitation and daily streamflow discharge: a historical perspective in a mid-atlantic subwatershed, *Landscape Ecology*, 17, 471-489.
- Karl, T. R. and W. E. Riebsame (1989) The impact of decadal fluctuations in mean precipitation and temperature on runoff: A sensitivity study over the United States. *Climatic Change* 15:423-47.
- Kashaigili, J.J. (2008) Impacts of land-use and land-cover changes on flow regimes of the

- Usangu wetland and the Great Ruaha River, Tanzania, *Physics and Chemistry of the Earth, Parts A/B/C*, 33(8-13), 640-647.
- Kennard, M.J., Pusey, B.J., Olden, J.D., Mackay, S.J., Stein, J.L., Marsh, N. (2010) Classification of natural flow regimes in Australia to support environmental flow management, *Freshwater Biology*, 55, 171-193.
- Kemp, W.M., Boynton, W.R., Adoli, J.E., Boesch, D.F., Boicourt, W.C., Brush, G., Cornwell, J.C., Fisher, T.R., Gilbert, P.M., Hagy, J.D., Harding, L.W., Houde, E.D., Kimmel, D.G., Miller, W.D., Newell, R.I.E., Roman, M.R., Smith, E.M., Stevenson, J.C. (2005) Eutrophication of Chesapeake Bay: historical trends and ecological interactions, *Marine Ecological Progress Series*, 303, 1-29.
- Kimmer, W.J. (2002) Physical, Biological, and Management Responses to Variable Freshwater Flow into the San Francisco Estuary, *Estuaries*, 25(6), 1275-1290.
- Knowles, N. (2002) Natural and management influences on freshwater inflows and salinity in the San Francisco Estuary at monthly to interannual scales, *Water Resources Research*, 38(12), 25-1-25-11.
- Krajewski, W.F., Ciach, G.J., Habib, E. (2003) An analysis of small-scale rainfall variability in different climatic regimes, *Hydrological Sciences Journal*, 48:2, 151-162, DOI: 10.1623/hysj.48.2.151.44694.
- Labet, D., Godderis, Y., Probst, J.L., Guyot, J.L. (2004) Evidence for global runoff increase related to climate warming, *Advances in Water Resources*, 27 (6), 631-642.
- Lakshmi, V., Jackson, T. J., Zehrhuhs, D. (2003) Soil moisture-temperature relationships: results from two field experiments, *Hydrological Processes*, 17, 3041-3057.
- Li, M., Xu, K., Watanabe, M., Chen, Z. (2007). Long-term variations in dissolved silicate, nitrogen, and phosphorus flux from the Yangtze River into the East China Sea and impacts on estuarine ecosystem, *Estuarine, Coastal, and Shelf Science*, 71, 3-12.
- Li, Z., Liu, M., Zhao, Y., Liang, T., Sha, J., Wang, Y. (2014) Application of Regional Nutrient Management Model in Tunxi Catchment: In support of the Trans-boundary Eco-compensation in Eastern China, *Soil, Air, Water*, 42, 1729-1739.
- Liu, M., Tian, H., Chen, G., Ren, W., Zhang, C., Liu, J. (2008) Effects of Land-Use and Land-Cover Change on Evapotranspiration and Water Yield in China During 1900-2000, *Journal of the American Water Resources Association*, 44(5), 1193-1207.
- Liu, X., Dai, X., Zhong, Y., Li, J., Wang, P. (2013) Analysis of changes in the relationship between precipitation and streamflow in the Yiluo River, China, *Theoretical and Applied Climatology*, 114(1), 183-191.
- Livingston, R.J., Niu, F., Lewis(III), F.G., and Woodsum, G.C. (1997) Freshwater Input to a gulf Estuary: Long-Term Control of Trophic Organization, *Ecological Applications*, 7(1), 277-299.
- Loureiro, S., Newton, A., Icely, J. (2005) Effects of nutrient enrichments on primary production in the Ria Formosa coastal lagoon (Southern Portugal), *Hydrobiologia*, 550(1), 29-45.
- Magilligan, F.J., Nislow, K.H. (2005) Changes in hydrologic regime by dams, *Geomorphology*, 71 (1-2), 61-78.
- Mechtensimer, S. and Toor, G.S. (2017) Septic Systems Contribution to Phosphorus in Shallow Groundwater: Field-Scale Studies Using Conventional Drainage Designs, *PLoS One*, 12(1).
- Miao, C., Ni, J. (2009) Variation of Natural streamflow since 1470 in the Middle Yellow River, China, *Int. J. Environ. Res. Public Health*, 6, 2849-2864.

- Moon, C. and Dunstan, W.M. (1990) Hydodynamic trapping in the formation of the chlorophyll a peak in turbid, very low salinity waters of estuaries, *Journal of Plankton Research*, 12 (2), 323-336.
- Montgomery, D.R. (2007) Soil erosion and agricultural sustainability, *PNAS*, 104(33), 13268-13272.
- Murrell, M.C., Hagy(III), J.D., Loes, E.M., and Greene, R.M. (2007) Phytoplankton Production and Nutrient Distributions in a Subtropical Estuary: Importance of Freshwater Flow, *Estuaries and Coasts*, 30(3), 390-402.
- Najjar, R.G., Pyke, C.R., Adams, M.B., Breitburg, D., Hershner, C., Kemp, M., Howarth, R., Mulholland, M.R., Paolisso M., Secor, D., Sellner, K., Wardrop, D., and Wood, R. (2010) Potential climate-change impacts on the Chesapeake Bay, *Estuarine, Coastal, and Shelf Science*, 86, 1-20.
- NCCGIA (North Carolina Center for Geographic Information & Analysis), 20070306, Type A Current Public Sewer Systems: NC Center for Geographic Information & Analysis, Raleigh, North Carolina.
- Neumann, B., Vafeidis, A.T., Zimmermann, J., Nicholls, R.J. (2015) Future Coastal Population Growth and exposure to sea level rise and coastal flooding- A Global Assessment, *PlosOne*, 10(6): e0131375. doi: 10.1371/journal.pone.0131375 .
- Nixon, S. W. (1995) Coastal marine eutrophication: a definition, social causes, and future concerns. *Ophelia*, 41, 199–219.
- Orth, R.J., Carrathers, T. J.B., Dennison, W.C., Duarte, C.M., Fourqurean, J.W., Heck, J.R., K.L., Hughes, A. R., Kendrick, G.A., Kenworthy, W.J., Olyarnik, S., Short, F.T., Waycott, M., Williams, S.L.(2006). A global crisis for seagrass ecosystems. *BioScience*, 56, 987-996.
- Pearl, H.S., Hall, N.S., Peierls, B.L., Rossignol, K.L., Joyner, A.R., Otten, T. (2013) Chapter 3: Develop and Deploy Microalgal Indicators as Measures of Water Quality, Harmful Algal Bloom Dynamics, and Ecosystem Condition, Final Technical Report to the Defense Coastal/Estuarine Research Program (DCERP1), RTI International, Research Triangle Park, NC
- Peierls, B.L., Hall, N.S., Paerl, H.W. (2012) Non-monotonic responses of phytoplankton biomass accumulation to hydrologic variability: A comparison of two coastal plain North Carolina estuaries, *Estuaries and Coasts*, 35(6), 1376-1392.
- Petersen, CR, Jovanovic, Le Maitre, DC, Grenfell, MC. (2017) Effects of land use change on streamflow and stream water quality of a coastal catchment, *Water SA*, 43(1), 139-152.
- Piehlner, M.F., Gold, A., Thompson, S. (2017) Chapter 5: MCBCL Tributary Creeks, DCERP2 Final Report.
- Piehlner, M.F., Gold, A., Thompson, S. (2017) Chapter 8: Climate and Land-Use Impacts on Exports of Carbon, Suspended Solids, and Nutrients from Coastal Subwatersheds, DCERP2 Final Report.
- Poff, L.N., Allen, D. J., Bain, M.B., Karr, J.R., Prestegard, K.L., Richter, B.D., Sparks, R.E., and Stromberg, J.C. (1997) The Natural Flow Regime, *BioScience*, 47(11), 769-784.
- Poff, L.N. and Ward, J.V. (1989) Implications of Streamflow Variability and Predictability for Lotic Community Structure: A Regional Analysis of Streamflow Patterns, *Canadian Journal of Fisheries and Aquatic Sciences*, 46, 1805-1817.
- Probst, J, Tardy, Y (1989) Global Runoff Fluctuations during the last 80 years in relation to world temperature change, *American Journal of Science*, 289, 267-285.

- Rabalais, N.N., Turner, R.E., Wiseman, W.J. (2001) Hypoxia in the Gulf of Mexico, *Journal of Environmental Quality*, 30, 320-329.
- Restrepo, J.D. and Kjerfve, B. (2000) Water Discharge and Sediment Load from the Western Slopes of the Colombian Andes with Focus on Rio San Juan, *The Journal of Geology*, 108(1), 17-33.
- Revelle, R. R. and P. E. Waggoner. (1983) Effects of carbon dioxide-induced climatic change on water supplies in the western United States. In *Changing Climate*, 419-32. Washington, DC: National Academy of Sciences, National Academy Press.
- Schoonover J.E, Lockaby B.G, Pan S. (2005) Changes in chemical and physical properties of stream water across an urban–rural gradient in western Georgia, *Urban Ecosystems*, 8, 107-124.
- Selker, J.S., Haith, D.A., Reynolds, J.E. (1990) Calibration and testing of daily rainfall Erosivity model. *Transactions of the American Society of Agricultural Engineers* 33(5): 1612-1618.
- Selman, M., Greenhaugl, S. Diaz,R., Sugg, Z. (2008) Eutrophication and Hypoxia in Coastal Areas: A Global Assessment of the State of Knowledge, WRI Policy Note Water Quality: Eutrophication and Hypoxia No.1, World Resources Institute, Washington D.C. <http://www.wri.org/map/world-hypoxic-and-eutrophic-coastal-areas>
- Sha,J., Liu, M., Wang, D., Swaney, DP, Wang, Y (2013) Application of the ReNuMa model in the Sha He river watershed: tool for watershed environmental management, *J Environ Manage*, 124, 40-50.
- Sha, J., Li, Z., Swaney, D., Hong, B., Wang, W., Wang, Y. (2014) Application of a Bayesian Watershed Model Linking Multivariate Statistical Analysis to Support Watershed-Scale Nitrogen Management in China, *Water Resources Management*, 28, 3681-3695.
- Short F.T., Burdick D.M. (1996) Quantifying eelgrass habitat loss in relation to housing development and nitrogen loading in Waquoit Bay, Massachusetts, *Estuaries*, 19,730–739.
- Shumway, S.E. (1990) A review of the effects of algal blooms on Shellfish and Aquaculture, *Journal of the World, Aquaculture Society*, 21, 64-104.
- Sklar, F.H. and Browder, J.A. (1998) Coastal environmental impacts brought about by alterations to freshwater flow in the gulf of Mexico, *Environmental management*, 22(4), 547-562.
- Solomon, S., Plattner, G.K., Knutti, R., Friedlingstein, P. (2009) Irreversible climate change due to carbon dioxide emissions, *PNAS*, 106(6), 1704-1709.
- Stogner, R.W. (2000). Trends in Precipitation and streamflow and changes in stream morphology in the Fountain Creek Watershed, Colorado, 1939-99, U.S. Geological Survey, Water-Resources Investigations Report 00-4130.
- Thronson, A. and Quigg, A. (2008) Fifty-Five Years of Fish Kills in Coastal Texas, *Estuaries and Coasts*, 31(4), 802-813.
- USDA-NASS (United States Department of Agriculture- National Agricultural Statistics Service. 2000-2008 Quick Stats U.S. and All States County Data- Crops database. United States Department of Agriculture, NationalAgricultural Statistics Service.
- Valiela, I., Collins,G., Lajtha,K., Geist,M., Seely,B., Brawley,J., Sham,C.H. (1997) Nitrogen loading from coastal watersheds to receiving estuaries: New method and application, *Ecological Applications*, 7, 358-380.
- Vanoni, V.A. (1975) Sedimentation Engineering, ASCE Manual and Reports on Engineering Practice Series, American Society of Civil Engineers, Reston, Va.

- Weller, D.E., Jordan, T.E., Correll, D.L. and Liu, Z-J (2003) Effects of Land-use Change on nutrient discharges from the Patuxent River Watershed, *Estuaries*, 26, 244-266.
- Weyers, H.S. (2013) New River monitoring near Gum Branch and Jacksonville, NC. Chapter 3 in: Final Monitoring Report to the Defense Coastal/Estuarine Research Program (DCERP1), RTI International, Research Triangle Park, NC.
- White, M.D. and Greer, K.A. (2006) The effects of watershed urbanization on the stream hydrology and riparian vegetation of Los Penasquitos Creek, California, *Landscape and Urban Planning*, 74(2), 125-138.
- Wooten, A., Sims, A., Aldreidge, H., Gray, G. (2017) Chapter 3: Development of Uniform Historical and Projected Climate Integrated Coastal Ecosystem Research, DCERP2 Final Report.
- Xin-Qiang, L., Lei, X., Hua, L., Miao-Miao, H., Yi-Chao, Q., Jin, L., Ze-Yu, N., Yu-Shi, Y., Yingxu, C. (2011) Influence of N fertilization rates, rainfall, and temperature on nitrate leaching from a rainfed winter wheat field in Taihu watershed, *Physics and Chemistry*, 36, 395-400.
- Yang, Z.F., Yan, Y. and Liu, Q. (2012) The relationship of streamflow-Precipitation-Temperature in the Yellow River Basin of China during 1961-200, *Procedia Environmental Sciences*, 13, 2336-2345.
- Zhang, L., Dawes, W.R., and Walker, G.R. (2001) Response of mean annual evapotranspiration To vegetation changes at catchment scale, *Water Resources Research*, 37(3), 701-708.

VITA

Shanna C. Williamson

Shanna was born and raised in the Bronx, NY. She attended the Foreign Language Academy of Global Studies (FLAGS) high school in the Bronx, NY. After graduating from high school, she attended Skidmore College and earned her B.A. in the Geosciences in 2014. In the fall of 2015, Shanna enrolled in the Master's program at William & Mary's School of Marine Science at the Virginia Institute of Marine Science.